INFLUENCE OF TREAD DEPTH ON WET SKID RESISTANCE OF TIRES

Albert Dijks, Delft University of Technology,
The Netherlands

Bald tires have lower skid resistance compared to tires with full tread depth. As could be expected tires with very low tread depths are reported to be more frequently involved in wet weather accidents. An overview of the legal requirements for the minimum value of the tread depth in several countries is given for car as well as truck and bus tires.

The influence of tread depth is not linear and depends strongly on vehicle speed and road surface characteristics. Measurements carried out in the U.K., Germany and the Netherlands are described and the different measuring methods are discussed. The measurements for car tires deal with the peak value of the braking force, the locked wheel value, as well as the side force coefficient.

The influence of tread depth of truck and bus tires has been investigated in the U.K. and the Netherlands as far as the braking force coefficients are concerned.

Especially in the lower tread depth range, the influence of tread depth on skid resistance is very important, for both car and truck tires. The results lead to the conclusion that a legislative minimum permissible tread depth can contribute to less skidding accidents. Although the level of this minimum value is theoretically somewhat arbitrary, practical considerations suggest that a minimum tread depth of 1,6 mm (2/32 inch) seems to be a sound limit.

Skid Resistance Coefficients

It is a well-known fact that the wet skid resistance of smooth tires is poor compared with tires with full tread depth (e.g. 1,2). The decrease in skid resistance however is not linearly dependant on the tread depth. Several investigations into the variation of wet skid resistance with tread depth have been carried out and will be discussed in this paper.

Wet skid resistance can be characterized by three coefficients, two braking force coefficients μ_{xm} and μ_{xb} and a side force coefficient μ_y.

The braking force coefficient and the side force coefficient are defined respectively as the instantaneous values of braking force and the side force, divided by the vertical load operating at that instant.

The three coefficients are:

$\mu_{xm} = (Fx/Fz)_{max}$, the maximum value of the braking force coefficient before locking.

$\mu_{xb} = (Fx/Fz)$, the average braking force coefficient when the wheel is locked.

$\mu_y = (Fy/Fz)$, the average side force coefficient at a slip angle exceeding, say, 8 deg.

Under different circumstances each of these coefficients is of overriding importance. A high value for μ_{xm} means that the brakes can be applied with force without the wheels locking. This situation is frequently encountered in nose-to-tail driving when it is often necessary to brake hard without there being any question of an emergency. A high μ_{xm} value is also of importance in connection with anti-locking devices. If, on the other hand, an emergency arises, the driver will usually brake as hard as he can, causing the wheels to lock and thereby endanger the stability of the vehicle. In this situation a high μ_{xb} value is required so as to achieve a short braking distance. On wet road surfaces μ_{xb} is always considerably lower than μ_{xm}. A high μ_y value is desirable when a driver wishes or needs to change direction and furthermore to promote stability during braking before the wheel locks.

Legislation

In many countries a minimum permissible tread depth has been fixed by law (table 1.)

Table 1. Legislative minimum tread dept in different countries.

	car tires	truck and bus tires
Austria	1.6	2
Belgium	1	1
Denmark	1[a]	1[a]
Finland	1	1
France	1[a]	1[a]
Germany	1[a]	1
Ireland	1	1
Italy	1	1
Japan	1.6	1.6
Netherlands	visible tread pattern	no visible carcass
Norway	1	1
Portugal	1	1
Spain	1	1
Sweden	1	1
Switzerland	1	1
United Kindom	1[a]	1[a]
USA	1.6	1.6
USSR	1	1

a. This minimum tread depth must be present throughout 3/4 of the width of the tread.

The European Tire and Rim Technical Organization (ETRTO) has recommended that the minimum tread depth of 1 mm should cover at least 3/4 of the width of the tread. The Economic Commission for Europe (ECE) of the United Nations recommends a minimum tread depth of 1 mm throughout the full width of the tread. In some countries however there is a tendency to require a higher value of the minimum tread depth.

The arguments put forward are generally more subjective rather than objective ones. A good case for a minimum permissible tread depth should be based upon an accident analysis in this respect. Unfortunately little reliable data are available on the question of involvement of tires with different tread depths at the sites of wet skid accidents.

Accident involvement of low tread depth tires

In Texas wet weather accidents were analyzed and the most important contributing factors determined (3). With respect to tire tread depth it was found that accident vehicles generally had less tread depth compared to the average vehicle in the study area. Rear wheels had generally remarkably lower tread depth compared to front wheels, 40% of the rear wheels had a tread depth less than 3,2 mm compared to about 25% of the front wheels.

Table 2. Percentages of inspected vehicles with low tread depths.

	wheel position							
	accident vehicle				sample vehicle			
	LF	RF	LR	RR	LF	RF	LR	RR
tread depth less than 1.6 mm	11	11	24	24	9	9	20	18
tread depth less than 3.2 mm	29	27	42	42	24	24	38	37

From table 2 it is clear that the percentage of low tread depth tires involved in wet weather accidents is significantly higher than the presence of these tread depths at random inspections. It seems that low tread depth is an important factor contributing to wet weather accidents.

A report of the Highway Safety Foundation in Ohio brings out the involvement of low tread depth tires in car accidents even more strongly (4). A statistical survey was carried out whereby relative accident involvement (R.I.) was determined. This was defined as follows:

R.I. = the percentage of tires with a particular tread depth of cars involved in accidents, divided by
the percentage of tires of this tread depth found during random inspection of vehicles.

It was established that on wet road surfaces tires with tread depths of less than 0.8 mm (1/32 inch) were involved in accidents to a far greater extent than tires with greater tread depths (Fig. 1).

Figure 1. Relative accident involvement as a function of tire tread depth.

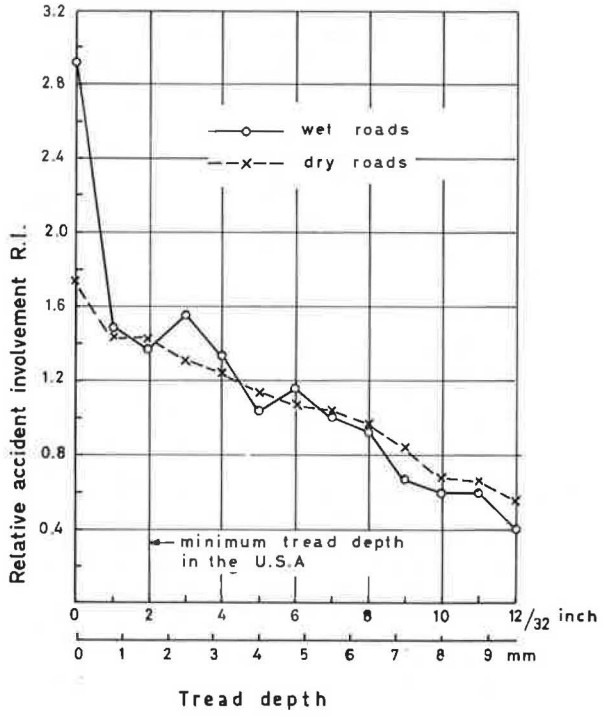

Also on dry surfaces the relative involvement in accidents of tires increase with decreasing tread depth, even though both the braking force coefficient and the side force coefficient usually increase under these circumstances. This implies that factors other than tread depth alone may also play a role in accidents. The sharply rising relative accident involvement on wet roads of tires with lower tread depths is explained by the much reduced braking force coefficients under these circumstances.

In this report an attempt has been made to calculate a cost-benefit factor in order to determine a critical value for the minimum tread depth. The method adopted is, however, very debatable. A distinction between trucks and busses and passenger cars was not made in the accident analyses before mentioned. The Ohio report deals only with car accidents.

Influence of tread depth of car tires on wet skid resistance

Only a few papers deal with the influence of tread depth on wet skid resistance. Some investigators have reported measurements of one tire on one specific road surface as a part of a general investigation of wet skid resistance (2,5). From these measurements no general conclusions could be drawn.

After 1970 more specific investigations into the influence of tread depth have been published; these were carried out in the United Kingdom, Germany and the Netherlands.

United Kingdom

In the United Kingdom the Road Research Laboratory has measured a particular type of cross-ply tire on six different road surfaces (6). The different tread depths were obtained by wearing the treads under normal traffic conditions. The drawback of this procedure is that the entire measurement was spread over an extended period of time, as a result of which measuring was done under widely varying weather conditions. It is true that adjustments were made so as to allow for variations in ambient temperature, by comparing the results with a reference bald tire, but it is our experience that measurements performed under widely differing weather conditions are difficult to interpret. Further limitations were that only one type of tire, a cross-ply tire, was tested, which is less interesting than a radial-ply tire, and that only braking force coefficients were measured.

The measurements were carried out by mounting the test tires on the front wheels of a high speed vehicle. The braking system had been modified such that the front brakes could be applied alone at a controlled rate until these wheels locked. The vehicle was allowed to coast immediately prior to the brake application so that the deceleration during coasting could be established. The additional deceleration during braking is a measure of the braking force. In the evaluation of the results the weight transfer to the front axle was taken into account.

A disadvantage of this method as far as the peak coefficient is concerned is that the deceleration of the vehicle is measured and the brake forces are averaged over the two tires. For the locked wheel values this would be true but as the peak braking force only appears for 1/10 of a second or less it is highly unlikely that this would occur exactly at the same time for both tires, on account of the dynamic wheel load variations. Therefore it may be expected that the μ_{xm} values measured in this way are lower than the true values for the individual tires. The measurements were carried out on 6 road surfaces ranging from smooth mastic asphalt to a rough and sharp aggregate, with a 5.60 $-_2$13 tire, load 3500 N, inflation pressure 180 kN/m^2. The water depth on all surfaces was about about 0.5 mm except on the mastic asphalt where a water layer with a depth of 1.1 mm was found. This was due to the road surface texture and drainage. The water depth was defined as the average depth of water standing above the aggregate of each of the test surfaces. The surfaces were maintained in a wetted condition using a spray bar facility. All the surfaces were part of a special test track.

In figure 2 some of the results are presented. Under certain conditions there appeared to be a very sharp drop in skid resistance when the tire wears to a tread depth below 1 or 2 mm. This effect is very pronounced in the peak values μ_{xm}.

Figure 2. Skid resistance as a function of tire tread depth. (Measurements in the U.K.)

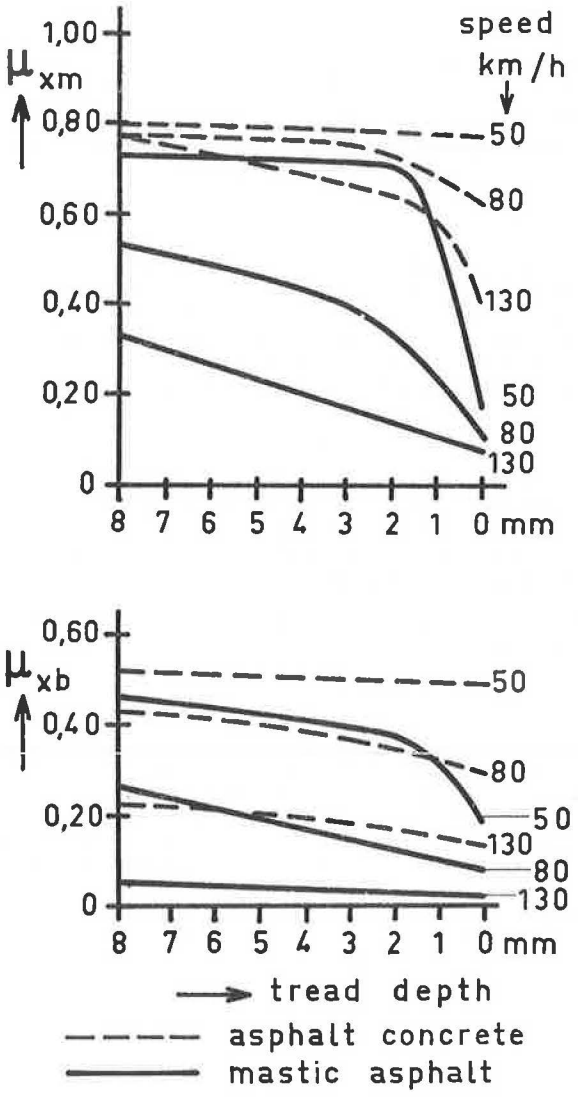

Germany

In Germany the influence of tire tread depth on the side force coefficient μ_y has been investigated (7). Two types of tires, a cross-ply and a radial ply tire have been tested.

The different tread depths were achieved by grinding down to the desired depth and subsequently running in the tires on public roads.

A normal car chassis was changed in such a way that during driving the front wheels could be set to slip angles in opposite directions in the range from -18 to +18 degrees. The side force was measured with the aid of a dynamometer mounted on the wheel. On a test track 3 surfaces were chosen from smooth concrete to a rather rough surface. On a racing track a very rough surface was available for the measurements. A water spray installation took care to maintain the calculated water depth of 1.5 mm, which may be considered as an extremely thick water layer. The tire sizes were 5.60-15 and 155SR15 with a vertical load of 2350 N and an inflation pressure of 150 kN/m^2.

Fig. 3 shows a typical set of test results. It can be seen that with decreasing tread depth the side force coefficient gradually decreases. There appears to be no particular point beyond which the μy value drops progressively. The radial-ply tire shows a remarkably higher μy value as compared to the cross-ply one.

Figure 3. Side force coefficients as a function of tire tread depth. (Measurements in W-Germany)

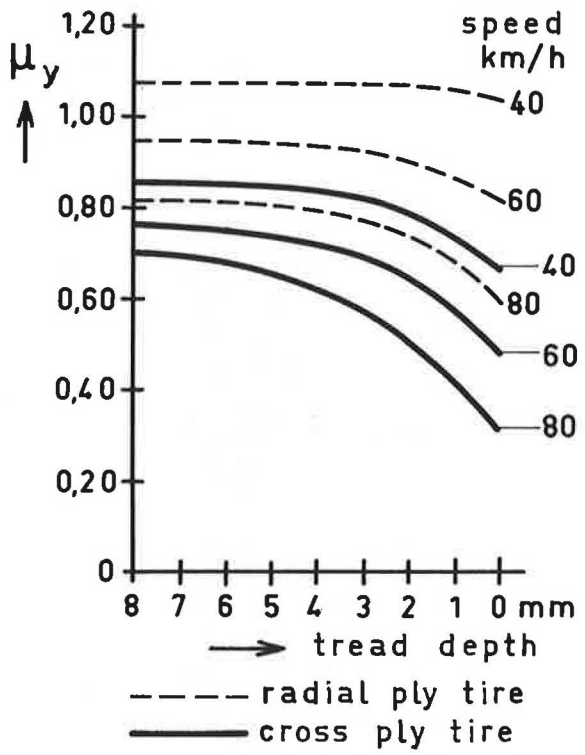

The Netherlands

Measurements of braking force coefficients as well as cornering force coefficients have been carried out by the Vehicle Research Laboratory of the Delft University (VRL). The VRL has a test trailer specially built for measuring tire traction characteristics (figure 4).

Figure 4. The VRL measuring trailer.

This trailer can steer, camber and brake the test tire. The tire to be measured is mounted on a five component measuring hub, placed in a frame (figure5).

Figure 5. Suspension of the measuring wheel.

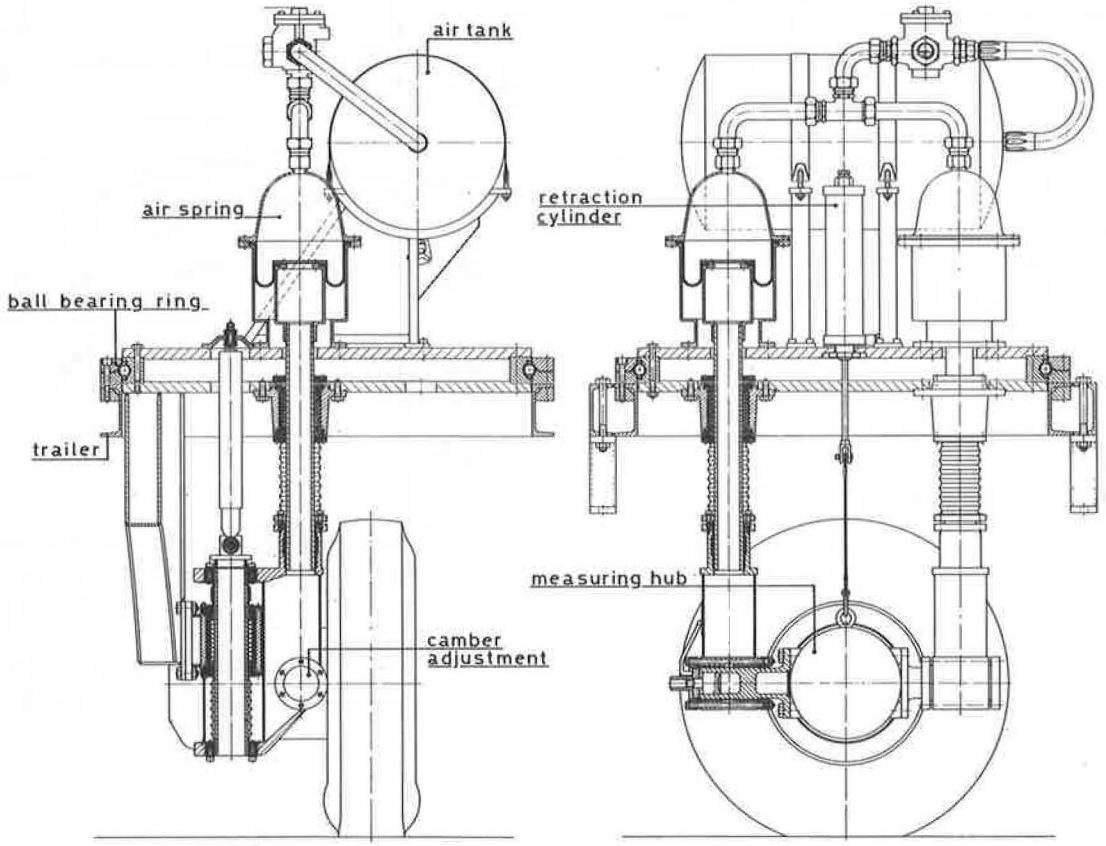

A similar frame is equipped with a dummy tire. Both frames can turn in opposite directions to provide slip angles to both tires. Resulting side forces on the trailer are in this way restricted to very low levels. The towing truck has a water tank and by means of air pressure water can be sprayed in front of the test tire. A special nozzle will give a thin flat water layer on the road. A disadvantage of this self supporting watering system is that the water is not at rest with respect to the road surface. But for measurements on public roads it is very difficult to install a water spray installation along the road sections to be measured.

The longitudinal force F_x and the side force F_y are continuously divided by the prevailing value of the vertical load F_z. An electronic device accomplishes this computation and the peak value of the braking force coefficient as well as the average value over the time span that the wheel is locked, are printed out. Also the side force coefficient is averaged over the time that the slip angle exceeds for instance 8 degrees.

Four types of car tires were examined: two textile radial tires and one steel cord radial, all of size 165 SR 13, and one cross-ply tire, size 5.90-13. Figure 6 shows the tread patterns of these tires. Five tires of each type were ground down to the desired tread depth.

Figure 6. Car tire tread patterns used for the measurements in the Netherlands.

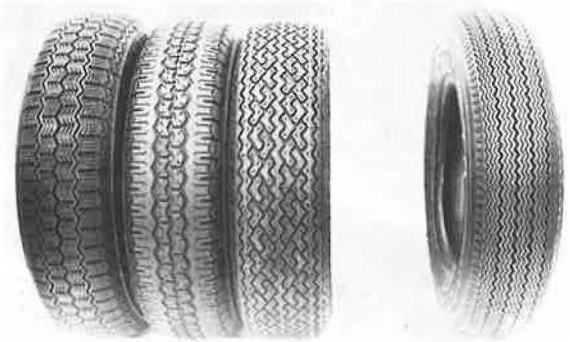

After grinding, the tires were run in for at least 500 kms. The tires were tested on two types of public road surfaces, A and B (figure 7), at a vertical load of 3300 N and inflation pressure of 180 kN/m^2.

friction device that does not measure a friction boundary condition - that is, the skiddometer measures peak braking (constant 0.13 braking slip); the General Motors (GM) trailer, either μ_{max} or μ_{skid} from a pulse braking technique; the Miles trailer, μ_{skid} from a pulse braking technique; and the DBV, μ_{skid} from a continuous locked-wheel braking technique. The Mu-Meter, on the other hand, measures cornering force developed on a tire at 7.5° yaw angle. At high pavement friction values, it cannot measure the peak friction boundary condition, whereas for low friction conditions, it may measure cornering force after the peak cornering-force value has been obtained, as shown in figure 26. The data in figure 26 were obtained from reference 31 (p. 654). These data suggest that if the yaw angle for maximum cornering force (limiting coefficient of friction) is exceeded, the cornering force (and cornering friction coefficient) is reduced as yaw angle is further increased. For the case of the Mu-Meter which measures cornering force at 7.5° yaw angle, this type of tire behavior may result in an overestimation of the slipperiness of the wet pavement defined by peak boundary friction conditions.

Aircraft/Ground-Vehicle Correlation

As with ground-vehicle/ground-vehicle correlation attempts, most aircraft/ground-vehicle correlation attempts try to relate the measured output of a friction device with some measured output of the aircraft from data obtained during joint testing of the device and aircraft on artificially wet runway surfaces. Typical aircraft/ground-vehicle relationships obtained from such test programs are shown in figures 27 (Mu-Meter, ref. 24) and 28 (DBV, refs. 11 and 25). Each friction device advocate claims good correlation between the device and the aircraft. For example, reference 26 states that the Mu-Meter may predict aircraft stopping performance within 10 to 15 percent if a correlation ranking system classifying runways surfaces into different texture groups is used. On the other hand, reference 11 states that the DBV can predict aircraft stopping performance within ±15 percent by using its prediction method. The tire friction prediction method (described earlier in the paper) offers another approach to show correlation between ground-vehicle and aircraft measurements of runway slipperiness.

Equation 5 may be modified to the form

$$\mu_{eff} = \eta \, \bar{Y}_R \, \mu_{dry} \qquad (8)$$

where

μ_{eff} effective braking friction coefficient realized by the aircraft through its antiskid braking system

$\bar{Y}_R$ runway tire-pavement drainage characteristic (hydroplaning parameter) determined by ground-vehicle friction test over ground speed range

μ_{dry} characteristic maximum aircraft tire friction coefficient on dry pavement

η antiskid braking system efficiency, μ_{eff}/μ_{max}

This method, using the DBV friction measuring device, is illustrated in figures 29 to 31. The correlation shown in the figures resulted from use of the arbitrarily selected antiskid braking system efficiency model depicted in figure 29 which is patterned after the one described in reference 32.

The data trends shown in figures 29 to 31 suggest that a ground-vehicle friction measuring device can be used to predict the effective friction coefficient an aircraft will develop on a wet runway providing the antiskid braking system efficiency of the aircraft is known. The data trends also suggest that each aircraft type has its own characteristic antiskid braking system efficiency which is dependent upon the landing gear, braking, and antiskid system design.

Summary of Correlation Results

The runway slipperiness research conducted since 1968 in the area of ground-vehicle/ground-vehicle and aircraft/ground-vehicle correlations has been reviewed and yields the following observations:

Ground-vehicle devices that test at constant speed do not correlate well with those devices that test over a speed range.

Ground-vehicle devices that test at constant speed can be correlated together as well as those that test over a speed range regardless of the tire operating mode during testing.

The DBV can be used to predict aircraft tire braking and cornering characteristics on wet runways. Other ground-vehicle devices have the potential to predict these tire characteristics as well if their test procedure is changed from a constant speed test to a speed range test similar to the DBV. Ground-vehicle devices that test at constant speed cannot predict aircraft tire braking and cornering friction coefficient on wet runways over the full take-off and landing speed range of aircraft.

Ground-vehicle and aircraft slipperiness measurements can be correlated. However, the precision of correlation is obtained from artificially wet runway test programs. The accuracy of prediction from the correlation may be degraded when runways are wet from natural rain (different water depths). Further, some of the older aircraft braking systems can allow locked-wheel operation during maximum braking operation on wet runways. The locked-wheel condition can result in reverted rubber hydroplaning which destroys the aircraft/ground-vehicle correlation. For these reasons, predictions of aircraft braking performance on wet runways from ground-vehicle devices should be employed only to provide guidance information to pilots.

Status of Runway Slipperiness Measurements

Standard USAF runway skid resistant tests.- Since November 1973, the Air Force Civil Engineering Center (AFCEC) has been measuring the skid resistance properties of airfields. Procedures for conducting the standard skid resistance tests are given in reference 33. This test requires that friction measurements be obtained by both the DBV and Mu-Meter when testing an airfield pavement. AFCEC feels that the friction data obtained from these friction measuring devices are complementary, and together they provide an adequate data base to evaluate the skid resistance of an airfield pavement. AFCEC intends to survey the skid resistance of all USAF runways in the United States and overseas on a periodic basis. AFCEC feels strongly that the concept of using an experienced, well-trained crew and standardized testing procedures for pavement skid

resistance evaluations offers many advantages. This concept requires the Air Force to purchase and maintain a minimum quantity of equipment and ensures that the testing is properly accomplished and documented. Results from this Air Force program are reported in references 28 and 34.

FAA Advisory Circular No. 150/5320-12.- FAA Airports Service issued FAA Advisory Circular No. 150/5320-12 on June 30, 1975 (ref. 35). This advisory circular provides guidance on methods that can be used to provide and maintain airport pavement surface friction characteristics. This guidance is intended for use by airport operators, engineering consultants, and maintenance personnel. This advisory circular does not purport to provide a means to predict aircraft stopping distance. For the requirements specified in this circular, FAA Airports Service requires a friction measuring device which

1. Can provide fast, accurate, and reliable friction values of airport pavement surfaces under varying climatic conditions
2. Can provide a continuous graph record of the pavement surface characteristics
3. Has minimal maintenance and recurring costs
4. Has a simple calibration technique
5. Indicates potential for hydroplaning conditions

This circular is worded carefully such that current friction measuring devices, the DBV for example, are not excluded from use in implementing the circular, although it is clear that the British Mu-Meter is the device favored by FAA Airports Service since it is the only device described in the circular. The advisory circular clearly indicates that its needs are met by a device which measures the relative friction of pavement surfaces and that this measurement of friction does not provide a means to predict aircraft stopping distance (determine how slippery the runway surfaces are for aircraft operation).

It is felt that issuance of this advisory circular by the FAA is a noteworthy step forward in providing guidance to install antihydroplaning runway surfaces at airports. However, the providing of relative friction measurements for engineering and maintenance purposes is secondary to the main objective of a friction evaluation which is to determine how slippery the runway surface is for aircraft operation.

Progress and Problems of Antihydroplaning Runway Surface Treatments

Both runway grooving and porous friction course (PFC) antihydroplaning runway surfaces were originated in England, as described in reference 36. Research on runway grooving in the United States started with NASA experiments in 1962 (reported in ref. 2). PFC pavement research in the United States was initiated by USAF (1972) and is reported in references 37 and 38.

Runway Grooving

Since 1956, approximately 160 runways have been grooved world-wide as indicated in tables 2 to 12. Figure 32 shows the development of grooved runways at U.S. civil airports since the first air carrier airport was grooved in 1967. For the past 3 years an average of 24 air carrier airport runways have been grooved each year. At this present rate, the 224 ILS runways 1524 m (5000 ft) or longer in length at U.S. air carrier airports will all be grooved by 1986. At the present time, six different methods are available for grooving runways, namely, diamond saws, abrasive (carborundum) saws, flails, plastic grooving with segmented drum, plastic grooving with wire comb, and plastic grooving with wire broom. The latter three methods can only be used for grooving portland cement concrete when it has been freshly laid and has not hardened or set up. The most popular grooving method is the diamond saw. Approximately 80 percent of the air carrier airport runways that have been grooved since 1967 have used this grooving method. The effectiveness of runway grooving as an antihydroplaning surface treatment is revealed by reviewing the DBV SDR data shown in tables 13 to 17. Tables 13 to 16 were obtained from reference 39. Table 17 shows data obtained from a recently completed FAA DBV trial application-runway friction calibration and pilot information program (ref. 40). Review of these data suggests that the greatest fraction benefit is realized from closed-spaced grooves that are cut 1/4 inch deep in the pavement with diamond saws. This result follows the trend reported in reference 27 where a 25 × 6 × 6 mm (1 × 1/4 × 1/4 in.) pattern was found to be superior to all other patterns studied with regard to preserving traction on wet or flooded runways. Plastic grooving treatments are considered to be an improvement over conventional ungrooved concrete surfaces but are inferior to diamond sawed grooves in both traction performance and water drainage (discussed in section "Flooding on Grooved Runways"). The uniformity of plastic grooving is poor compared with diamond sawed grooves as shown by comparing figures 5 and 6 with figure 33. The data presented in figure 34 compare the traction performance of plastic grooving using a wire comb technique (ref. 41) with other antihydroplaning pavement surface treatments. These data confirm the traction trends just discussed.

The major problem encountered with grooved runways is the chevron cutting of aircraft tires during the touchdown phase of aircraft landings on grooved runways. (See fig. 35.) This problem is discussed in detail in reference 39 and has been studied in reference 42. The civil airlines in the United States at the present time do not consider chevron cutting to be a serious operational problem to their jet transport fleet. It should be noted that the aircraft tire industry has been working in close cooperation with aircraft operators on the chevron cutting problem. During the past 5 years, the aircraft tire industry has developed new tread rubber compounds and tread designs that significantly reduce the degree of chevron cutting on aircraft tires experienced on grooved runways. In this regard, American Airlines reports that over the past 4 years, the number of landings per tire change on its jet transport fleet has increased by 50 percent. During this time period, the number of grooved runways at air carrier airports has increased from 37 to 107. The slipperiness of grooved runways is increased when heavy rubber deposits coat touchdown areas, but this problem is easily corrected by rubber removal treatments (discussed later). Some asphaltic concrete runways have suffered collapsed grooves in trafficked areas. This type of problem is usually created by grooving the asphaltic concrete shortly after the runway has been paved and before the asphaltic concrete has cured properly.

Porous Friction Course

The first PFC surface treatment in the United States was at the Dallas Naval Air Station in 1971

as indicated in table 18. The growth of the PFC surface treatment at U.S. civil airports (through 1975) is shown in figure 36. Over the past 3 years (1973 to 1975), an average of seven air carrier airport runways per year have been given this antihydroplaning pavement surface treatment. Figure 34 shows that this surface is definitely superior in traction qualities over conventional ungrooved concrete and ranks with pavement grooving in this regard as reported in reference 19. PFC has a high storage volume to prevent runway flooding when rain first commences but does not have the free flowing drainage features common to grooved runways. Consequently (as discussed earlier in the paper), PFC surface treatments are not believed to be as effective as grooved pavements, especially those cut with diamond saws, in preventing runway flooding during sustained, high rainfall rate precipitation conditions.

A major problem that has been reported for PFC pavements is the difficulty of removing rubber from contaminated touchdown areas of the runway. AOCI (Airport Operators Council International) reports that the PFC surface at Johannesburg had to be replaced because rubber deposits could not be removed from the surface. A similar problem has been encountered at Denver Stapleton Airport where the rubber deposits could be removed only through the use of a flailing machine and high-pressure water-blast equipment. It should be stressed that the PFC surface treatments at U.S. airports have not been installed long enough at the present time to report realistically on the durability and maintainability of this type pavement surface.

Runway Rubber Deposits and Their Removal

NASA, USAF, and FAA studies (tables 13 to 17) show that the most slippery runway segments are usually those located in aircraft touchdown areas which become covered with heavy rubber deposits. The reduced macro/microtexture of the pavement surface (fig. 37) resulting from rubber deposits makes the runway much more susceptible to dynamic and viscous hydroplaning during times of rain. The dramatic runway traction loss suffered as a consequence is illustrated by figure 38. Reference 11 points out that wheel spin-up at touchdown on the Roswell smooth concrete runway (SDR = 2.17 to 2.75 for DBV, B-737, and L-1011) required as much as 2 seconds. From a comparison of figures 13 and 38, the predicted aircraft tire friction coefficient μ_{skid} available to spin the tire up on the rubber coated ungrooved runway at MIA runway 9R/27L (SDR = 4.62) is found to be much less than at Roswell. Consequently, wheel spin-up times may take from 6 to 8 seconds on this wet, contaminated surface. As a consequence, pilots may apply wheel braking before the wheels are spun up with the result that the antiskid braking system fails to perform properly and poor braking, poor directional control along with reverted rubber skidding may occur for the aircraft. (See refs. 8 and 11.) Obviously, runway rubber deposits pose a distinct threat to the operational safety of aircraft during landings and take-offs in adverse weather. This paper has pointed out that ground vehicles which test pavements utilizing a constant speed technique cannot predict the runway slipperiness resulting to aircraft from this effect. Therefore, the DBV, which has a demonstrated capability to perform this measurement, should be the only device permitted to assess this runway condition. Only when test procedures have been changed and the devices correlated or calibrated satisfactorily with the DBV, should other devices be allowed to measure the effects of rubber deposits on runway slipperiness for aircraft operation.

Review of the data contained in tables 13 to 17 and figures 37 and 38 indicates that grooved runways are much less affected by rubber deposits than ungrooved runways and may require less frequent cleaning. Several methods for cleaning runways of rubber deposits are available and discussed in reference 40. One of the most effective means is by high-pressure water blast as shown in figures 39 and 40.

Concluding Remarks

This paper has reviewed the runway slipperiness research performed in the United States and abroad over the time period 1968 to the present. This review suggests that this research has been extremely fruitful with the following tangible benefits resulting to the aviation community:

1. A better understanding of the hydroplaning phenomena
2. A method for predicting aircraft tire performance on wet runways from a ground-vehicle braking test
3. The runway rubber deposit problem has been defined as one of the most serious threats to aircraft operational safety during landings and take-offs in adverse weather; at the same time, methods have been developed which can remove runway rubber deposits so that runway traction is effectively restored to uncontaminated levels
4. Pavement grooving has fulfilled its promise as a runway surface treatment that minimizes runway flooding during heavy rainstorms and produces nearly dry aircraft braking and cornering performance under wet runway conditions
5. Porous friction course surface treatments are nearly as effective as pavement grooving, but further research and time are required to assess the effects of rubber deposits (and removal), durability, and maintainability of this surface treatment

Finally, it is hoped that this report on the status of runway slipperiness research will stimulate the aviation community and the Federal Regulatory Agencies into a rapid implementation program to utilize the technological advances this research has produced and to improve airport runway safety.

References

1. Galloway, Bob M.; Schiller, Robert E., Jr.; and Rose, Jerry G.: The Effects of Rainfall Intensity, Pavement Cross Slope, Surface Texture, and Drainage Length on Pavement Water Depths. Res. Rep. No. 138-5, Texas Transp. Inst., Texas A&M Univ., May 1971.
2. Horne, Walter B.; Yager, Thomas J.; and Taylor, Glenn R.: Review of Causes and Alleviation of Low Tire Traction on Wet Runways. NASA TN D-4406, 1968.
3. Horne, Walter B.; and Dreher, Robert C.: Phenomena of Pneumatic Tire Hydroplaning. NASA TN D-2056, 1963.
4. Aircraft Accident Report - Caribbean Atlantic Airlines, Inc.; Douglas DC-9-31, N938PR; Harry S. Truman Airport, Charlotte Amalie, St. Thomas, Virgin Islands; August 12, 1969. Rep. No. NTSB-AAR-70-23, Sept. 16, 1970.

5. Aircraft Accident Report - Piedmont Airlines; Boeing 737, N751N; Greensboro, N.C.; October 28, 1973. Rep. No. NTSB-AAR-74-7, May 22, 1974.
6. Horne, Walter B.; and Joyner, Upshur T.: Determining Causation of Aircraft Skidding Accidents or Incidents. Paper presented at the 23rd Annual International Air Safety Seminar, Flight Safety Foundation, Inc. (Washington, D.C.), Oct. 1970.
7. Horne, Walter B.: Elements Affecting Runway Traction. [Preprint] 740496, Soc. Automat. Eng., Apr.-May 1974.
8. Horne, Walter B.; McCarty, John L.; and Tanner, John A.: Some Effects of Adverse Weather Conditions on Performance of Airplane Antiskid Braking Systems. NASA TN D-8202, 1976.
9. Merritt, Leslie R.: Impact of Runway Traction on Possible Approaches to Certification and Operation of Jet Transport Aircraft. [Preprint] 740497, Soc. Automot. Eng., Apr.-May 1974.
10. Cantu, A. G.; and Chernick, B. E.: Model 737 Data - FAA Evaluation of Proposed Landing Certification Rules. Doc. No. D6-43078, Boeing Co., Dec. 1973.
11. Merritt, Leslie R.: Concorde Landing Requirement Evaluation Tests. Report No. FAA-FS-160-74-2, 1974.
12. Gough, V. E.: Discussion of Paper by D. Tabor, Frottement en Caoutchouc, Rev. Ge'n du Caoutchouc, vol. 36, 1959.
13. Frictional and Retarding Forces on Aircraft Tyres. Part I: Introduction. Eng. Sci. Data Item No. 71025 with ammendment A, R. Aeronaut. Soc., Aug. 1972.
14. Leland, Trafford J. W.; Yager, Thomas J.; and Joyner, Upshur T.: Effects of Pavement Texture on Wet-Runway Braking Performance. NASA TN D-4323, 1968.
15. Lander, F. T. W.; and Williams, T.: The Skidding Resistance of Wet Runway Surfaces With Reference to Surface Texture and Tyre Conditions. RRL Rep. LR 184, Road Res. Lab., British Minist. Transp., 1968.
16. Rose, F. G.; Gallaway, R. M.; and Hankins, K. D.: Macrotexture Measurements and Related Skid Resistance at Speeds From 20 to 60 Miles Per Hour. Highway Research Record no. 341, 1970, pp. 33-45.
17. Horne, Walter B.: Skidding Accidents on Runways and Highways Can Be Reduced. Astronaut. & Aeronaut., vol. 5, no. 8, Aug. 1967, pp. 48-55.
18. Expansion of Flight Simulator Capability for Study and Solution of Aircraft Directional Control Problems on Runways. Phase I - Final Report. Rep. MDC A3304 (Contract NAS1-13378), McDonnell Aircraft Co., Mar. 15, 1975. (Available as NASA CR-145084.)
19. Yager, Thomas J.; Phillips, W. Pelham; Horne, Walter B.; and Sparks, Howard C. (appendix D by R. W. Sugg): A Comparison of Aircraft and Ground Vehicle Stopping Performance on Dry, Wet, Flooded, Slush-, Snow-, and Ice-Covered Runways. NASA TN D-6098, 1970.
20. Smiley, Robert F.; and Horne, Walter B.: Mechanical Properties of Pneumatic Tires With Special Reference to Modern Aircraft Tires. NASA TR R-64, 1960. (Supersedes NACA TN 4110.)
21. Horne, Walter B.; and Tanner, John A.: Joint NASA-British Ministry of Technology Skid Correlation Study - Results From American Vehicles. Pavement Grooving and Traction Studies, NASA SP-5073, 1969, pp. 325-359.
22. Sugg, R. W.: Joint NASA-British Ministry of Technology Skid Correlation Study - Results From British Vehicles. Pavement Grooving and Traction Studies, NASA SP-5073, 1969, pp. 361-409.
23. Anon.: Model L-1011-1 (Base Aircraft) Landing Performance Report for FAA Evaluation of Concorde SST Special Condition 25-43-EU-12. Rep. No. LR 26267, Lockheed Aircraft Corp., Jan. 14, 1974.
24. Sugg, R. W.: The Development and Testing of the Runway Friction Meter MK 1 (Mu-Meter). AF/542/043, British Minist. Def., June 1972.
25. Merritt, L. R.: Analysis of Tests Conducted by the French Ministry of Armed Forces Flight Test Center for the Service Technique Aeronautique (STAe) Utilizing a Caravelle 116 Aircraft and a Diagonal Braked Vehicle (DBV). Rep. No. FS-160-75-2, FAA, Oct. 1975.
26. Blanchard, J. W.: An Analysis of the B727 and DC9 Trials on Wet Runways With the Mu-Meter and Diagonal Braked Vehicle (DBV). Civil Aviat. Auth. (London), Dec. 1974.
27. Yager, Thomas J.: Comparative Braking Performance of Various Aircraft on Grooved and Ungrooved Pavements at the Landing Research Runway, NASA Wallops Station. Pavement Grooving and Traction Studies, NASA SP-5073, 1969, pp. 35-65.
28. Williams, John H.: Analysis of the Standard USAF Runway Skid Resistance Tests. AFCEC-TR-75-3, U.S. Air Force, May 1975.
29. Nussbaum, Peter J.; Hiering, William A.; and Grisel, Charles R.: Runway Friction Data for 10 Civil Airports as Measured With a Mu-Meter and Diagonal Braked Vehicle. Rep. No. FAA-RD-72-61, July 1972.
30. Horne, Walter B.: Results From Studies of Highway Grooving and Texturing at NASA Wallops Station. Pavement Grooving and Traction Studies, NASA SP-5073, 1969, pp. 425-464.
31. Van Eldik Thieme, H. C. A.: Cornering and Camber Experiments. Mechanics of Pneumatic Tires, Samuel K. Clark, ed., NBS Monogr. 122, U.S. Dep. Commer., Nov. 1971, pp. 631-693.
32. Preston, O. W.; Kibbee, G. W.; Muroyama, R. H.; and Storley, R. A.: Development of a Basic Methodology for Predicting Aircraft Stopping Distance on a Wet Runway. Rep. No. FAA-RD-70-62, Mar. 1971.
33. Ballentine, George D.; and Compton, Phil V.: Procedures for Conducting the Air Force Weapons Laboratory Standard Skid Resistance Test. AFWL-TR-73-165, U.S. Air Force, Sept. 1973.
34. AFCEC Pavement Surface Effects Team: Runway Skid Resistance Survey Report. Air Force Civil Eng. Center, U.S. Air Force, 1975. Production FLT/Test Instln, AF Plant 42, Palmdale, California, Mar. 1975.
Norton AFB, California, Apr. 1975.
March AFB, California, Apr. 1975.
Vandenberg AFB, California, Apr. 1975.
Williams AFB, California, Apr. 1975.
Davis Monthan AFB, Arizona, Apr. 1975.
Reese AFB, Texas, May 1975
Carswell AFB, Texas, May 1975.
Dyess AFB, Texas, May 1975.
Webb AFB, Texas, May 1975.
Laughlin AFB, Texas, May 1975.
Randolph AFB, Texas, May 1975.
Barksdale AFB, Louisana, May 1975.
Yokota AFB, Japan, Aug. 1975.
Elmendorf AFB, Alaska, Aug. 1975.

35. Methods for the Design, Construction, and Maintenance of Skid Resistant Airport Pavement Surfaces. AC No. 150/5320-12, FAA, June 30, 1975.
36. Martin, F. R.: Pavement Surface Treatments at Airports in Great Britain. Pavement Grooving and Traction Studies, NASA SP-5073, 1969, pp. 235-278.
37. Tomita, Hisao; and Forrest, J. B.: Porous Friction Surfaces for Airfield Pavements. AFWL-TR-74-177, U.S. Air Force, May 1975.
38. Compton, Phil V.; and Hargett, Emil R.: Skid-Resistance Evaluation of Seven Antihydroplaning Surfaces. AFWL-TR-74-64, U.S. Air Force, May 1974.
39. Horne, Walter B.; and Griswold, Guy D.: Evaluation of High Pressure Water Blast With Rotating Spray Bar for Removing Paint and Rubber Deposits From Airport Runways, and Review of Runway Slipperiness Problems Created by Rubber Contamination. NASA TM X-72797, 1975.
40. Merritt, Leslie R.: Trial Application-Runway Friction Calibration and Pilot Information Program. Rep. No. AFS-160-76-1, FAA, Aug. 19, 1976.
41. Marlin, Eugene C.; and Horne, Walter B.: Plastic (Wire-Combed) Grooving of a Slip-Formed Concrete Runway Overlay at Patrick Henry Airport - An Initial Evaluation. Paper presented at the Southeastern Airport Managers Association (Fort Lauderdale, Fla.), Nov. 1973.
42. Byrdsong, Thomas A.; McCarty, John Locke; and Yager, Thomas J.: Investigation of Aircraft Tire Damage Resulting From Touchdown on Grooved Runway Surfaces. NASA TN D-6690, 1972.

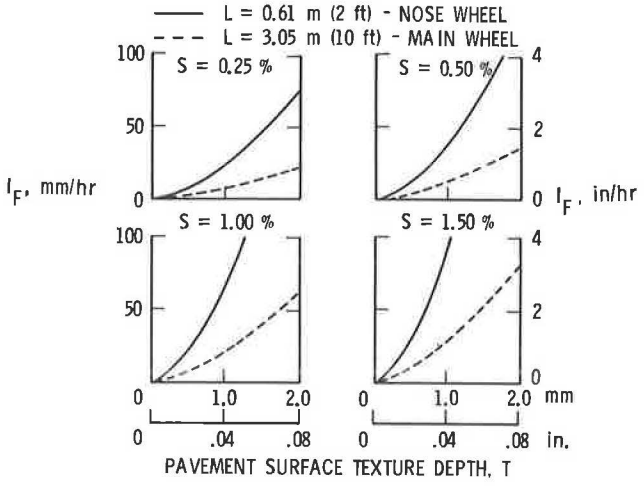

Figure 1. Rainfall rate required to flood tire path on conventional runway surfaces. Landings on center line.

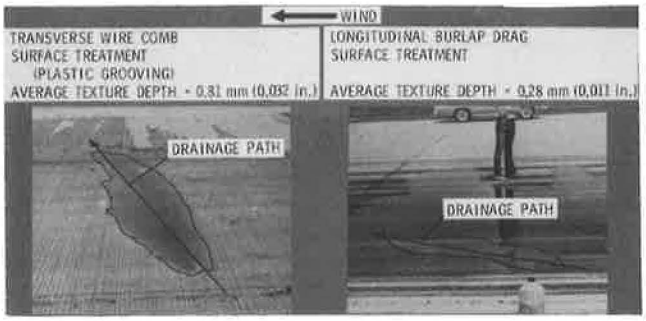

Figure 2. Water drainage from concrete runway at PHF. Water truck wetting; runway 6/24; wind from 60° at 10 knots.

Figure 3. Space shuttle landing facility at KSC.

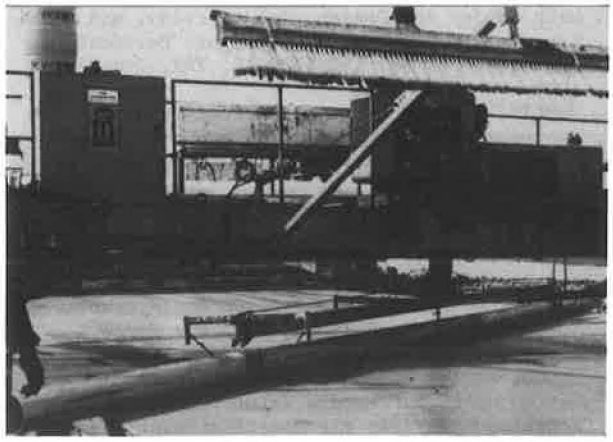

Figure 4. Space shuttle landing facility at KSC with slip-form paving equipment, leveling tube, and longitudinal broom.

Figure 5. Space shuttle landing facility at KSC with pavement grooving machine (diamond blades).

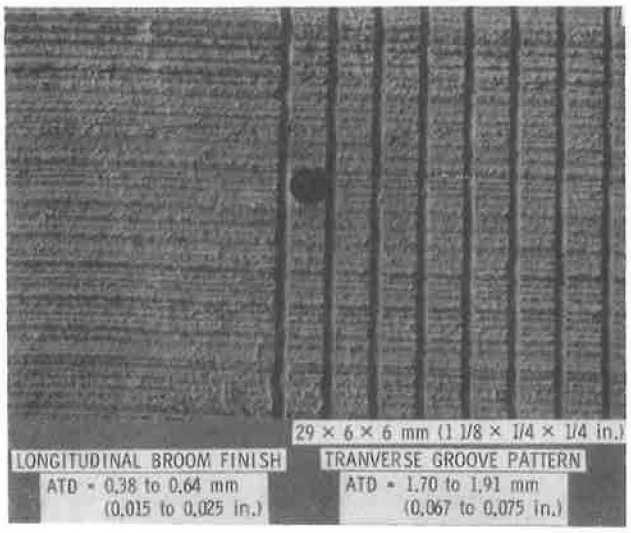

Figure 6. Concrete runway surface texture of space shuttle landing facility at KSC.

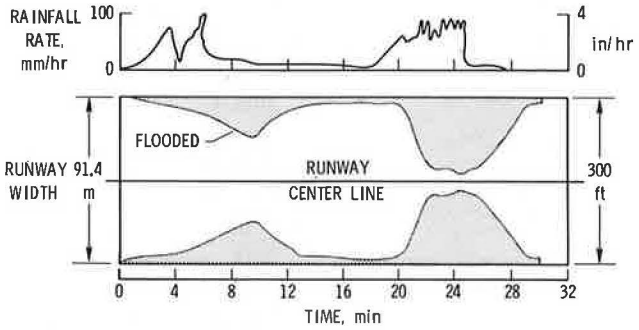

Figure 7. Surface flooding on space shuttle grooved runway during thunderstorm 6/20/76.

Figure 8. Water drainage from grooved and ungrooved asphalt. Grooving pattern, 38 × 6 × 6 mm (1-1/2 × 1/4 × 1/4 in.).

Figure 10. B-737 tire reverted rubber skid patch after 1.8 km (6000 ft) locked-wheel skid on wet smooth concrete.

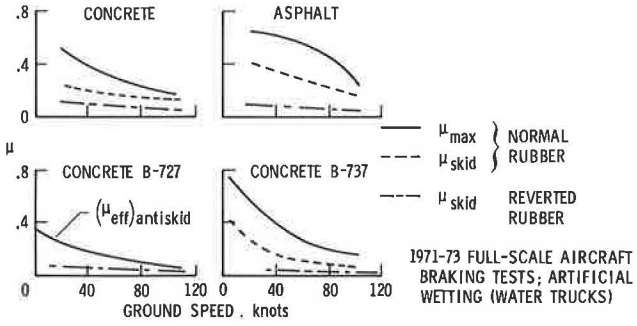

Figure 11. Aircraft flight test confirmation of reverted rubber hydroplaning 1965 NASA track; 32 × 8.8 aircraft tire; flooded runway.

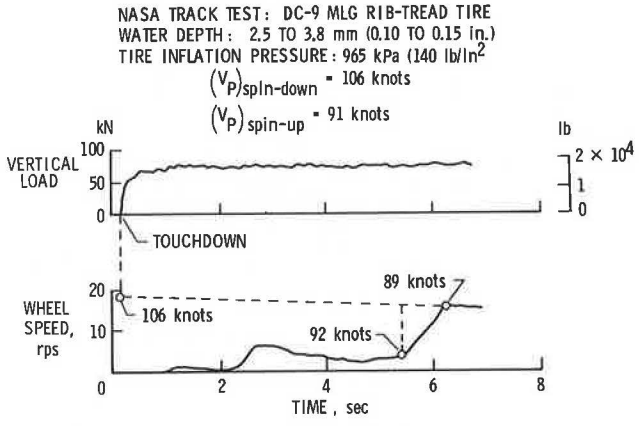

Figure 9. Delayed wheel spin-up at touchdown on flooded runway.

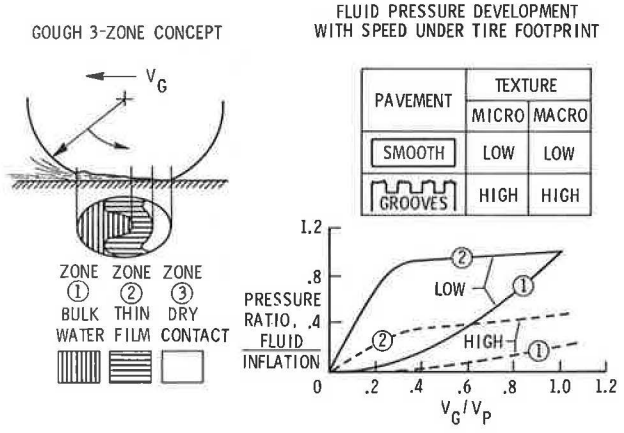

Figure 12. NASA model for combined viscous and dynamic tire hydroplaning.

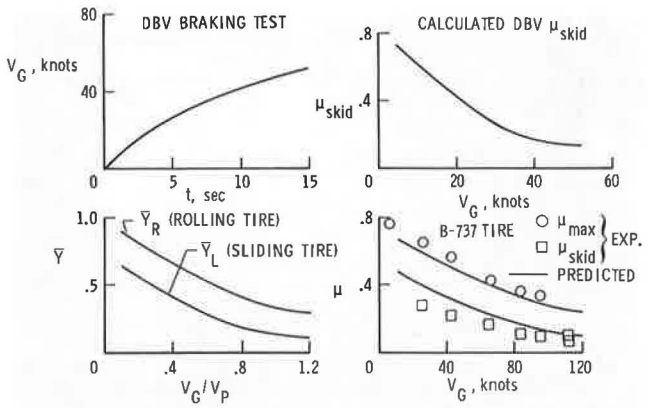

Figure 13. Prediction of aircraft tire friction coefficient from ground-vehicle braking test on a wet runway by NASA theory.

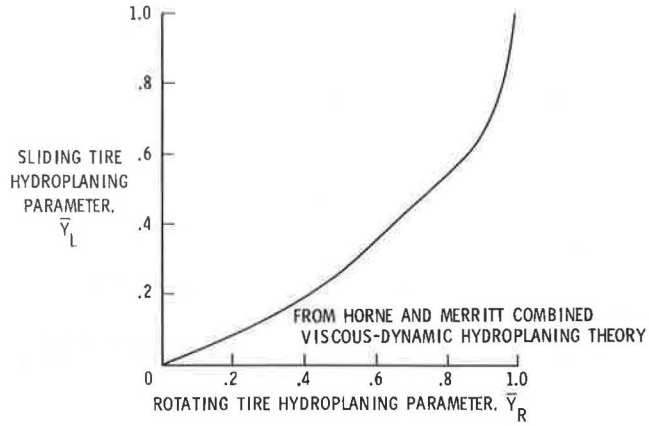

Figure 14. Empirically derived relationship between sliding ($\bar{Y}_L$) and rotating ($\bar{Y}_R$) tire hydroplaning parameters.

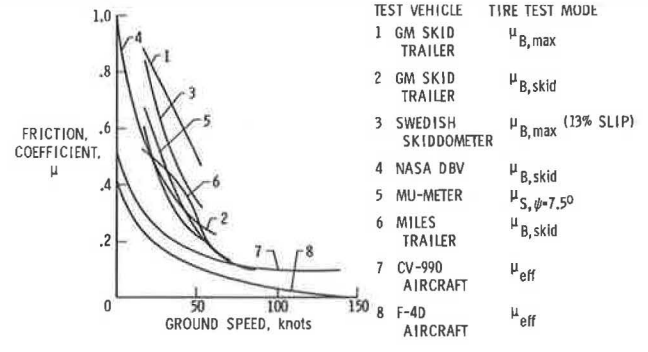

Figure 15. Aircraft/ground-vehicle correlation problem for wet and puddled smooth concrete surface.

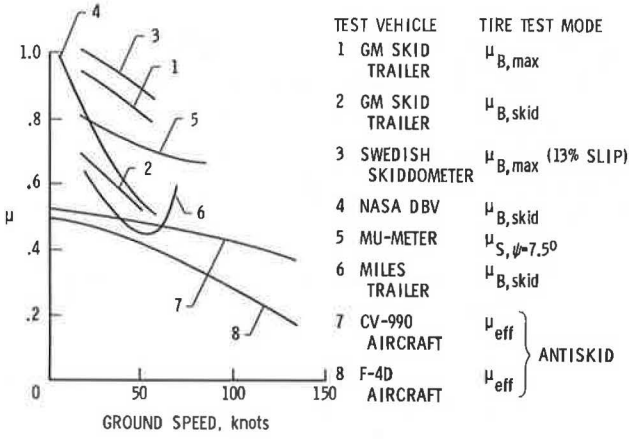

Figure 16. Aircraft/ground-vehicle correlation problem for wet and puddled grooved asphalt.

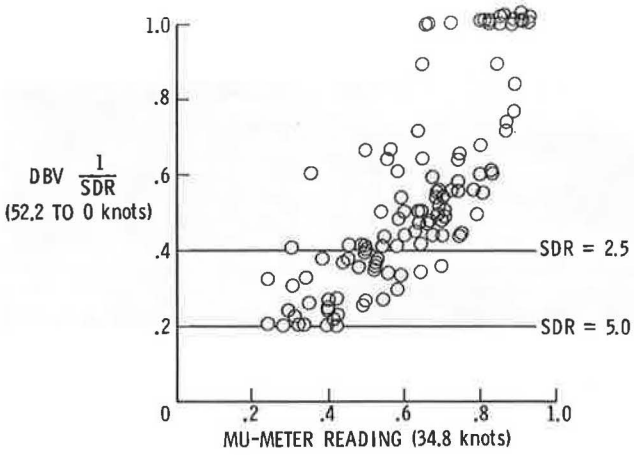

Figure 17. DBV/Mu-Meter relationship found by USAF tests (ref. 28).

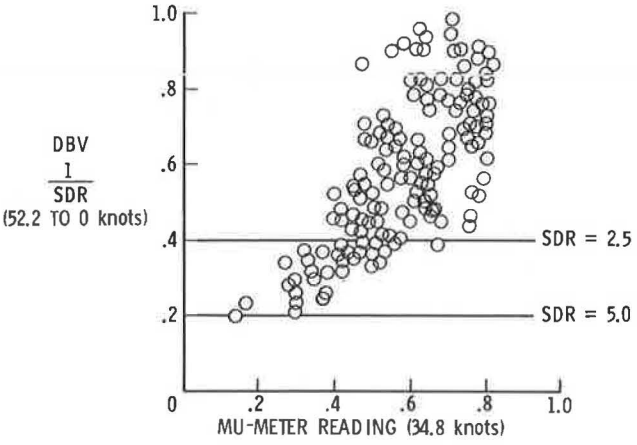

Figure 18.- DBV/Mu-Meter relationship found by FAA tests on 31 runways.

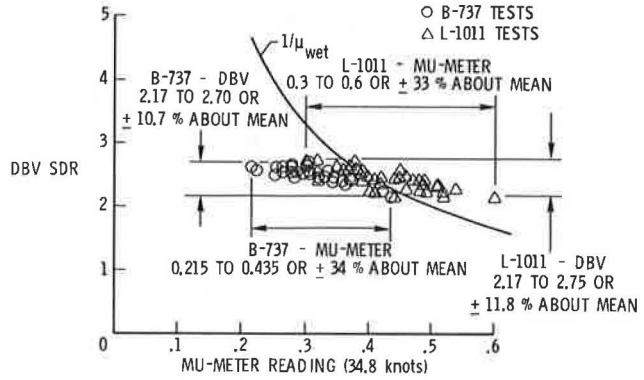

Figure 19. Comparison of NASA DBV with Mu-Meter.

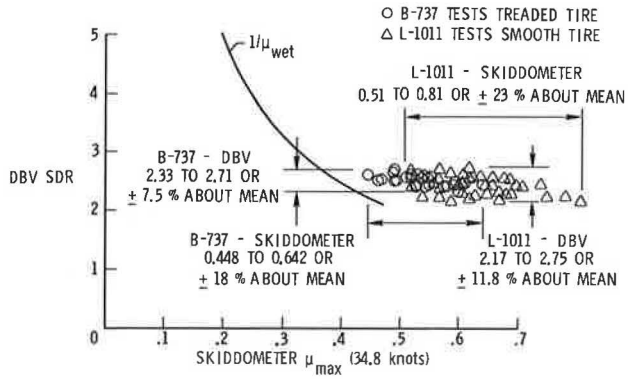

Figure 20. Comparison of NASA DBV with skiddometer.

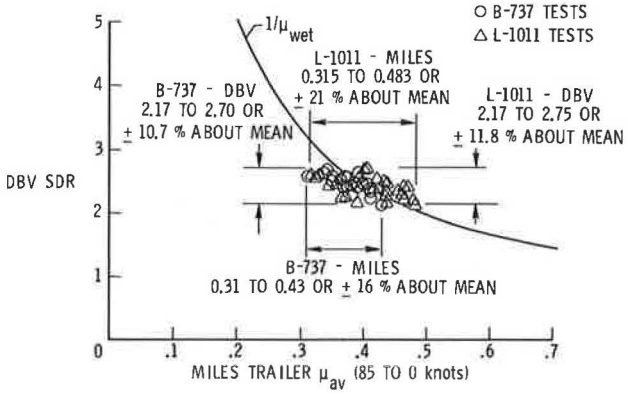

Figure 21. Comparison of NASA DBV with Miles trailer.

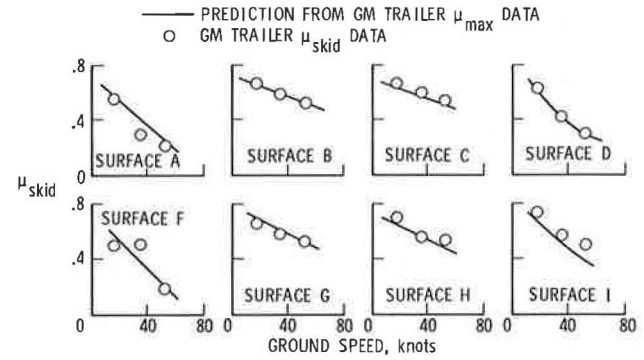

Figure 22. Prediction of GM trailer μ_{skid} from GM trailer μ_{max} data. ASTM smooth tread tire; data from reference 22.

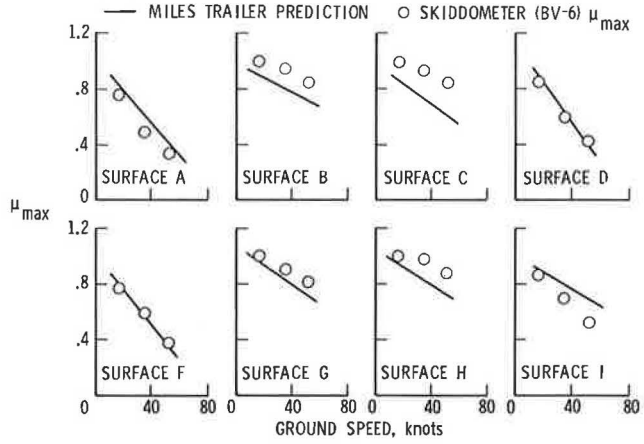

Figure 23. Prediction of skiddometer μ_{max} from Miles trailer μ_{skid} data. Data from references 21 and 22.

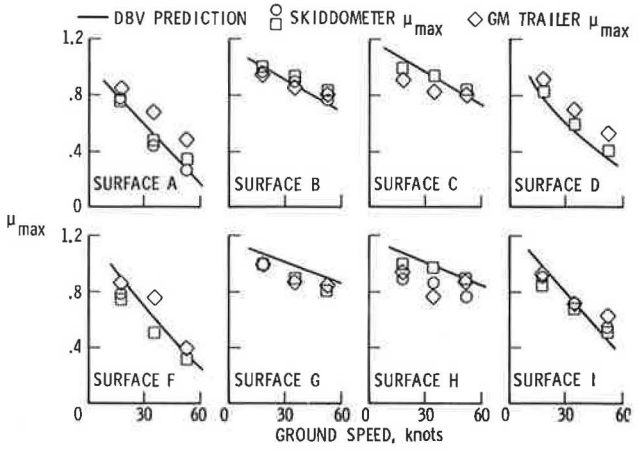

Figure 24. Prediction of skiddometer and GM trailer μ_{max} from DBV μ_{skid} data. Data from references 21, 22, and 30.

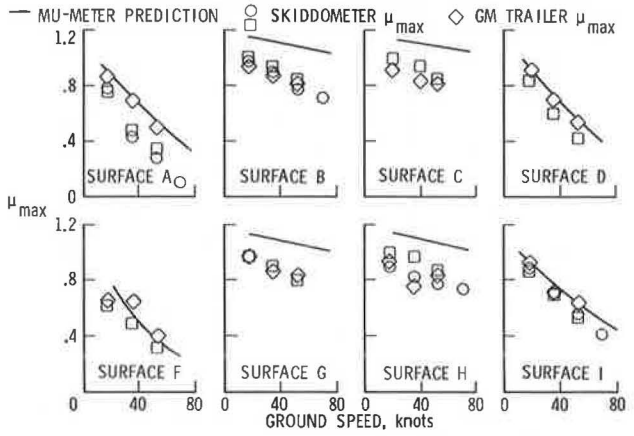

Figure 25. Prediction of skiddometer and GM trailer μ_{max} from Mu-Meter friction reading (ψ = 7.5°). Data from references 21, 22, and 30.

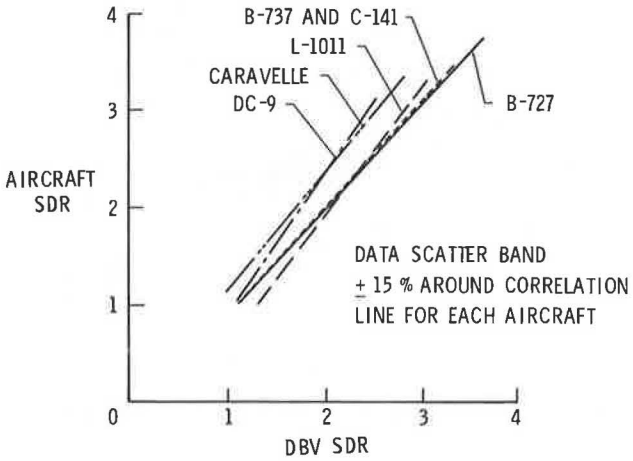

Figure 28. Aircraft/DBV correlation on wet runways for different jet transports.

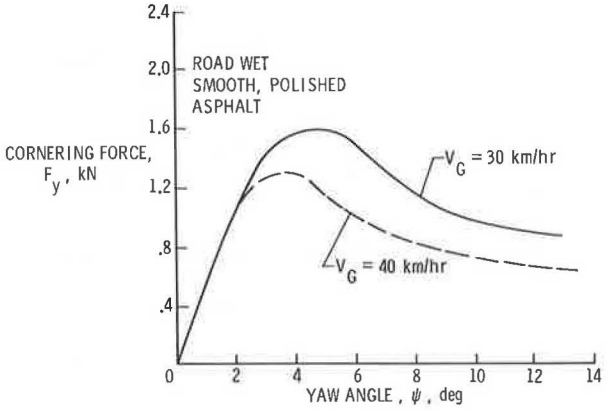

Figure 26. Effect of ground speed on cornering-force-yaw-angle relationships for 5.60-13 automobile tire. F_z = 2.70 kN; p = 167 kPa; from reference 31.

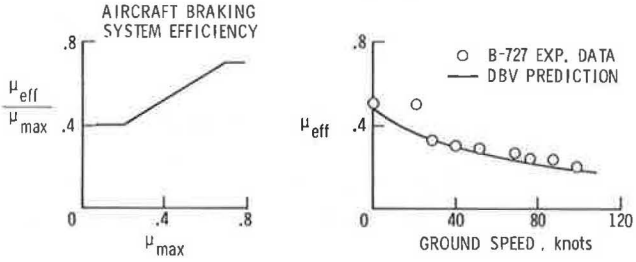

Figure 29. Prediction of aircraft braking performance on wet runway from DBV braking test. JFK runway 4R/22L; grooved concrete; water truck wetting.

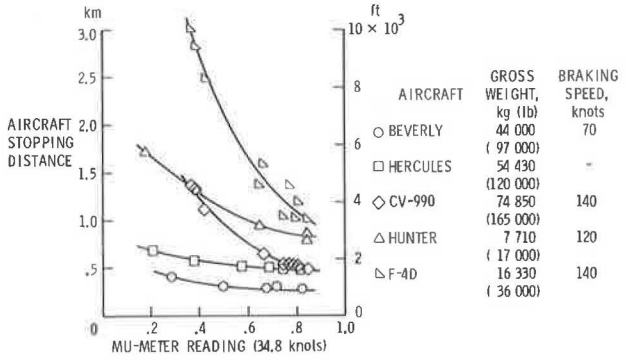

Figure 27. Mu-Meter correlation with aircraft stopping distances on wet surfaces.

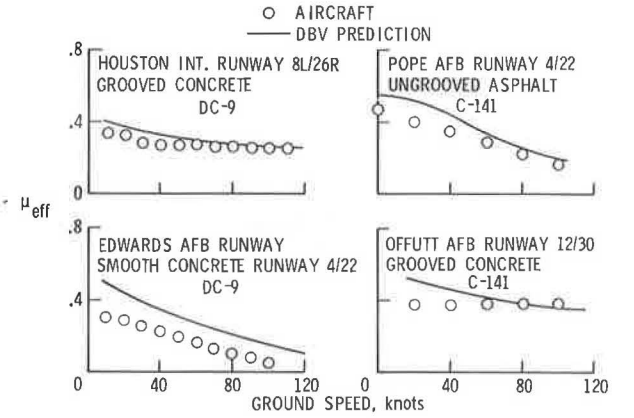

Figure 30. Prediction of aircraft braking performance on wet runways from DBV braking test for DC-9 and C-141 jet transports.

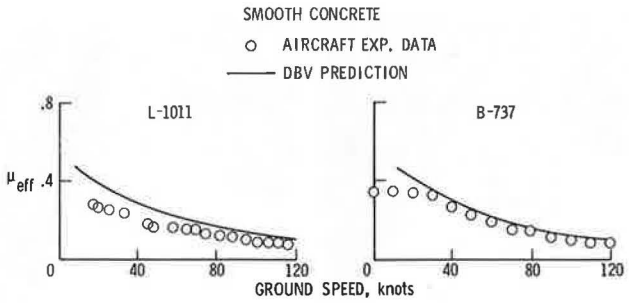

Figure 31. Prediction of aircraft braking performance on wet runway from DBV braking test for B-737 and L-1011 jet transports. Roswell runway 3/21; smooth concrete.

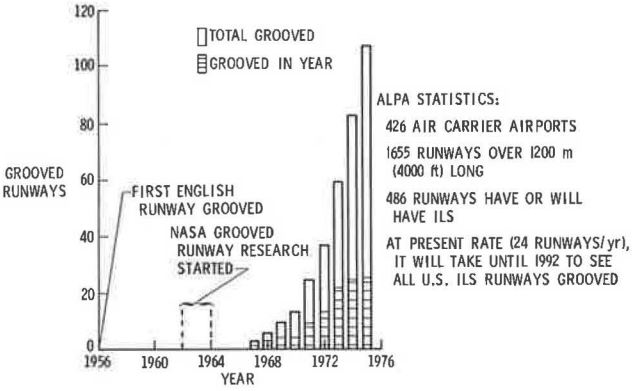

Figure 32. Number of grooved runways at U.S. air carrier airports.

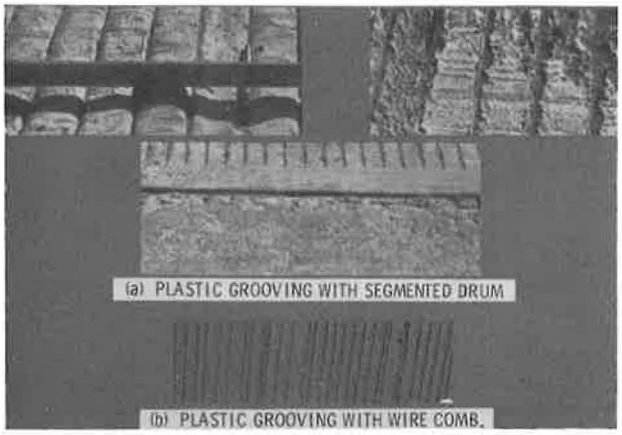

Figure 33. Examples of plastic grooving of Portland cement concrete.

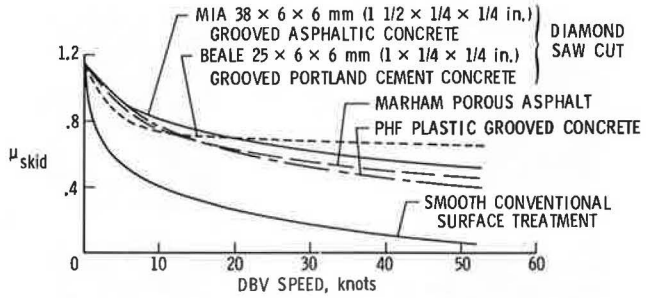

Figure 34. Wet skid resistance of several new type runway surface treatments. Artificial wetting.

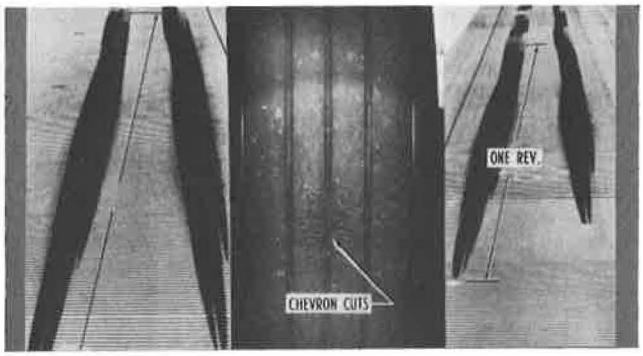

Figure 35. Tire damage from wheel spin-up at touch-down on dry grooved runway. Wallops grooved concrete; groove pattern, 25 × 6 × 6 mm (1 × 1/4 × 1/4 in.); CV-990 jet transport MLG tire, size 41 × 15.0-18; p = 1102 kPa (160 lb/in^2); V_G = 125 knots.

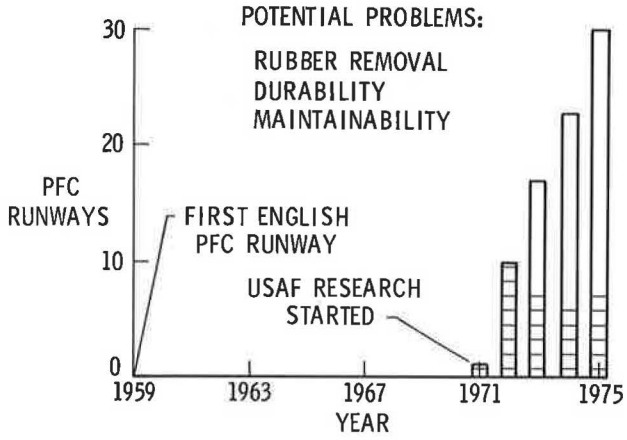

Figure 36. Number of porous friction course runways at U.S. air carrier airports.

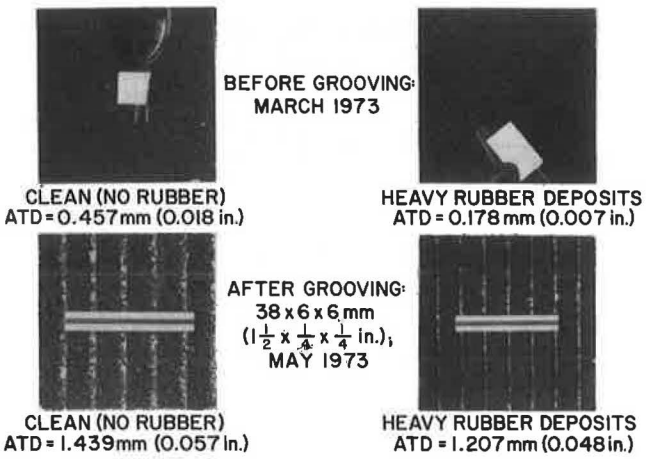

Figure 37. Effect of rubber deposits on runway surface texture.

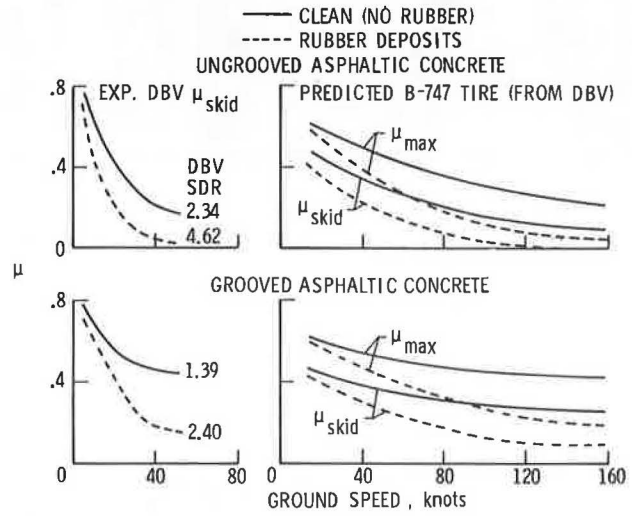

Figure 38. Effect of rubber deposits on runway traction before and after grooving.

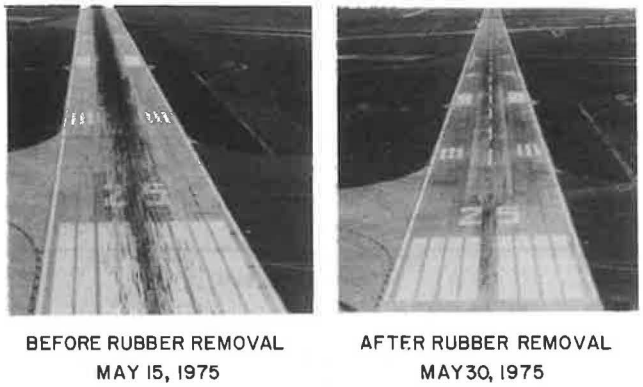

Figure 39. Approach end of LAFB runway 25 before and after rubber removal by high-pressure water blast.

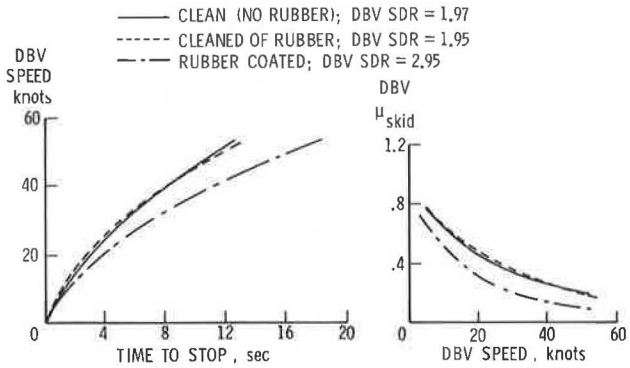

Figure 40. Effect of rubber removal by high-pressure water blast on runway traction. LAFB runway 25; May 1975.

Device	μ_{dry}	p	
		kPa	lb/in^2
DBV (ASTM E-249 smooth tread tire)	1.15	165	24
DBV (ASTM E-524 smooth tread tire)	1.20	165	24
Mu-Meter	0.84	69	10
Miles trailer	1.15	138	20
Skiddometer model BV-6 (ASTM E-249 smooth tread tire). . .	1.15	165	24

Table 1. Tire characteristics of friction measuring devices

Airport	Country	Runway	Surface	Grooving technique	Groove pattern, P × W × D	
					mm	in.
A (1956) - M	UK	N/A	AC	T-F	25 × 3 × 3	1 × 1/8 × 1/8
B (1957) - M	UK	N/A	AC	T-F	25 × 3 × 3	1 × 1/8 × 1/8
C (1960) - M	UK	N/A	AC	T-F	25 × 3 × 3	1 × 1/8 × 1/8
D (1960) - M	UK	N/A	AC	T-F	25 × 3 × 3	1 × 1/8 × 1/8
E (1960) - M	UK	N/A	PCC	T-F	25 × 3 × 3	1 × 1/8 × 1/8
F (1961) - M	UK	N/A	AC	T-CS	25 × 3 × 3	1 × 1/8 × 1/8
Manchester (1961) - C	UK	N/A	AC	T-F	25 × 3 × 3	1 × 1/8 × 1/8
NASA LaRC (1964) - C	USA	Research track	AC	T-DS	25 × 3 × 3	1 × 1/8 × 1/8
			PCC	L-DS	25 × 6 × 6	1 × 1/4 × 1/4
Manchester (1965) - C	UK	N/A	AC	T-F	25 × 3 × 3	1 × 1/8 × 1/8
Ubon (1966) - M	USA	N/A	PCC	T-DS	51 × 6 × 6 (Skip 610)	2 × 1/4 × 1/4 (Skip 24)
Udorn (1966) - M	USA	N/A	PCC	T-DS	51 × 6 × 6 (Skip 610)	2 × 1/4 × 1/4 (Skip 24)
NASA LaRC (1966) - C	USA	Research track	PCC	T-F	25 × 3-9 × 3	1 × 1/8-3/8 × 1/8
					38 × 3-9 × 3	1 1/2 × 1/8-3/8 × 1/8
					51 × 3-9 × 3	2 × 1/8-3/8 × 1/8
				T-DS	25 × 3-9 × 6	1 × 1/8-3/8 × 1/4
					38 × 3-9 × 6	1 1/2 × 1/8-3/8 × 1/4
					51 × 3-9 × 6	2 × 1/8-3/8 × 1/4

Table 2. Grooved runways constructed during 1956-1966

Airport	Country	Runway	Surface	Grooving technique	Groove pattern, P × W × D	
					mm	in.
Bien Hoa - M	USA	N/A	PCC	T-DS	51 × 6 × 6 (Skip 610)	2 × 1/4 × 1/4 (Skip 24)
Birmingham - C	UK	N/A	AC	T-F	25 × 3 × 3	1 × 1/8 × 1/8
Beale AFB - M	USA	14/32	PCC	T-DS	25 × 6 × 6	1 × 1/4 × 1/4
John F. Kennedy - C	USA	4R/22L	PCC	T-DS	38 × 10-5 × 3	1 1/2 × 3/8-3/16 × 1/8
Kansas City Mun. - C	USA	18/36	PCC/AC	T-DS	25 × 3 × 6	1 × 1/8 × 1/4
NASA Wallops - C	USA	4/22	PCC/AC	T-DS	25 × 6 × 6	1 × 1/4 × 1/4
Washington Nat. - C	USA	18/36	AC	T-DS	25 × 3 × 3	1 × 1/8 × 1/8

Table 3. Grooved runways constructed during 1967

Airport	Country	Runway	Surface	Grooving technique	Groove pattern, P × W × D	
					mm	in.
Atlanta Mun. - C	USA	9R/27L	PCC	T-DS	32 × 10-3 × 6	1 1/4 × 3/8-1/8 × 1/4
Chicago-Midway - C	USA	13R/31L	PCC	T-DS	32 × 6 × 6	1 1/4 × 1/4 × 1/4
Chicago-Midway - C	USA	4R/22L	PCC	T-DS	32 × 6 × 6	1 1/4 × 1/4 × 1/4
Seymour-Johnson AFB - M	USA	8/26	PCC/AC	T-DS	51 × 6 × 6 (Skip 610)	2 × 1/4 × 1/4 (Skip 24)
Tempelhof (Ger.) - M	USA	9R/27L	AC	T-DS	38 × 10 × 10	1 1/2 × 3/8 × 3/8

Table 4. Grooved runways constructed during 1968

Airport	Country	Runway	Surface	Grooving technique	Groove pattern, P × W × D	
					mm	in.
Boston Logan - C	USA	N/A	AC	T-DS	25 × 6 × 6	1 × 1/4 × 1/4
Charleston (W.Va.) - C	USA	5/23	PCC/AC	T-DS	32 × 6 × 6	1 1/4 × 1/4 × 1/4
Chicago O'Hare - C	USA	9L/27R	PCC/AC	T-DS	32 × 6 × 6	1 1/4 × 1/4 × 1/4
Dallas Love Field - C	USA	13R/31L	PCC	T-DS	32 × 6 × 6	1 1/4 × 1/4 × 1/4
Offutt AFB - M	USA	12/30	PCC	T-DS	32 × 6 × 6	1 1/4 × 1/4 × 1/4
Wellington - C	New Zealand	N/A	AC	T-DS	25 × 3 × 3	1 × 1/8 × 1/8

Table 5. Grooved runways constructed during 1969

Airport	Country	Runway	Surface	Grooving technique	Groove pattern, P × W × D	
					mm	in.
Bankok	Thailand	N/A	PCC	T-DS	51 × 6 × 6	2 × 1/4 × 1/4
Dallas Love Field - C	USA	13L/31R	AC	T-DS	38 × 10 × 6	1 1/2 × 3/8 × 1/4
Harry S. Truman - C	USA	9/27	PCC/AC	T-DS/CS	38 × 10 × 6	1 1/2 × 1/4 × 1/4
Kadena - M	USA	N/A	PCC/AC	T-DS	32 × 6 × 6	1 1/4 × 1/4 × 1/4
Nashville Met. - C	USA	2L/20R	AC	T-DS/CS	51 × 6 × 6	2 × 1/4 × 1/4
Nashville Met. - C	USA	13/31	PCC/AC	T-DS/CS	32 × 6 × 6	1 1/4 × 1/4 × 1/4
Orly - C	France	N/A	PCC	T-DS	N/A	N/A
Port Hardy - C	Canada	N/A	AC	T-DS	25 × 6 × 6	1 × 1/4 × 1/4
Shemya - M	USA	10/28	AC	T-DS	32 × 6 × 6	1 1/4 × 1/4 × 1/4

Table 6. Grooved runways constructed during 1970

Airport	Country	Runway	Surface	Grooving technique	Groove pattern, P × W × D	
					mm	in.
Boston Logan - C	USA	4R/22L	AC	T-DS	57 × 6 × 6	2 1/4 × 1/4 × 1/4
Chicago O'Hare - C	USA	4R/22L	PCC	T-DS	32 × 6 × 6	1 1/4 × 1/4 × 1/4
Houston Int. - C	USA	8L/26R	PCC	T-DS	51 × 6 × 6	2 × 1/4 × 1/4
Kaitak - C	Hong Kong	13/31	PCC/AC	T-DS	44 × 6 × 6	1 3/4 × 1/4 × 1/4
Kunsan - M	USA	17/35	PCC	T-DS	32 × 6 × 6	1 1/4 × 1/4 × 1/4
LaGuardia - C	USA	4/22	AC	T-DS	38 × 10-5 × 5	1 1/2 × 3/8-3/16 × 3/16
LaGuardia - C	USA	13/31	AC	T-DS	38 × 10-5 × 5	1 1/2 × 3/8-3/16 × 3/16
Memphis Int. - C	USA	17R/35L	PCC	T-PGWB	N/A	N/A
Newark - C	USA	4L/22R	AC	T-DS	38 × 10-5 × 5	1 1/2 × 3/8-3/16 × 3/16
San Diego Lindberg - C	USA	9/27	PCC	T-DS	25 × 6 × 6	1 × 1/4 × 1/4
Springfield (Ill.) - C	USA	4/22	PCC	T-DS	32 × 6 × 6	1 1/4 × 1/4 × 1/4
Tampa Int. - C	USA	18L/36R	PCC	T-PGWB	N/A	N/A

Table 7. Grooved runways constructed during 1971

Airport	Country	Runway	Surface	Grooving technique	Groove pattern, P × W × D	
					mm	in.
Baton Rouge - C	USA	4/22	PCC	T-PG	51 × 6 × 6	2 × 1/4 × 1/4
Boston Logan - C	USA	4R/22L	AC	T-DS	57 × 8 × 6	2 1/4 × 5/16 × 1/4
Cincinnati - C	USA	18/36	AC	T-DS	38 × 6 × 6	1 1/2 × 1/4 × 1/4
Cincinnati - C	USA	9R/27L	PCC	T-DS	38 × 6 × 6	1 1/2 × 1/4 × 1/4
Denver Stapleton - C	USA	17L/35R	PCC	T-DS	51 × 6 × 6	2 × 1/4 × 1/4
Detroit Metro. - C	USA	3L/21R	PCC	T-DS	32 × 6 × 6	1 1/4 × 1/4 × 1/4
Minneapolis - C	USA	4/22	PCC	T-DS	51 × 6 × 6	2 × 1/4 × 1/4
Oklahoma City - C	USA	17R/35L	PCC	T-PG	25 × 13 × 13	1 × 1/2 × 1/2
Omaha Eppley Field - C	USA	14R/32L	AC	T-DS	32 × 6 × 6	1 1/4 × 1/4 × 1/4
Osan - M	USA	9/27	PCC	T-DS	32 × 6 × 6	1 1/4 × 1/4 × 1/4
Plattsburg - M	USA	17/35	PCC	T-DS	38 × 6 × 6	1 1/2 × 1/4 × 1/4
Shaw - M	USA	4L/22R	PCC	T-DS	51 × 6 × 6 (Skip 610)	2 × 1/4 × 1/4 (Skip 24)
Springfield (Mo.) - C	USA	1/19	PCC	T-DS	51 × 6 × 6	2 × 1/4 × 1/4
St. Paul Holman - C	USA	12/30	AC	T-DS	32 × 6 × 6	1 1/4 × 1/4 × 1/4
Waterloo Mun. - C	USA	12/30	PCC	T-DS	32 × 6 × 6	1 1/4 × 1/4 × 1/4
Washington Nat. - C	USA	18/36	AC	T-DS	32 × 6 × 6	1 1/4 × 1/4 × 1/4

Table 8. Grooved runways constructed during 1972

Airport	Country	Runway	Surface	Grooving technique	Groove pattern, P × W × D	
					mm	in.
Allentown - C	USA	6/24	AC	T-DS	32 × 6 × 6	1 1/4 × 1/4 × 1/4
Atlanta Int. - C	USA	9R/27L	PCC	T-PGWC	N/A	N/A
Baltimore Int. - C	USA	10/28	AC	T-DS	32 × 6 × 6	1 1/4 × 1/4 × 1/4
Baltimore Int. - C	USA	15/33	AC	T-DS	32 × 6 × 6	1 1/4 × 1/4 × 1/4
Charles DeGaulle - C	France	N/A	PCC	T-DS	N/A	N/A
Clarksburg - C	USA	3/21	AC	T-DS	51 × 6 × 6	2 × 1/4 × 1/4
Cleveland Hopkins - C	USA	5R/23L	AC	T-DS	38 × 6 × 6	1 1/2 × 1/4 × 1/4
Dallas/Ft. Worth - C	USA	17L/35R	PCC	T-DS	38 × 6 × 6	1 1/2 × 1/4 × 1/4
Dallas/Ft. Worth - C	USA	17R/35L	PCC	T-DS	38 × 6 × 6	1 1/2 × 1/4 × 1/4
Dallas/Ft. Worth - C	USA	13L/31R	PCC	T-DS	38 × 6 × 6	1 1/2 × 1/4 × 1/4
Gainsville Mun. - C	USA	10/28	AC	T-DS	38 × 6 × 6	1 1/2 × 1/4 × 1/4
Griffiss - M	USA	15/33	PCC	T-DS	51 × 6 × 6	2 × 1/4 × 1/4
Huntington - C	USA	12/30	AC	T-DS	32 × 6 × 6	1 1/4 × 1/4 × 1/4
Jacksonville Int. - C	USA	7/25	AC	T-DS	51 × 6 × 6	2 × 1/4 × 1/4
Lafayette (Ind.) - C	USA	10/28	AC	T-DS	32 × 6 × 6	1 1/4 × 1/4 × 1/4
LaGuardia - C	USA	13/31	AC	T-DS	38 × 10-5 × 5	1 1/2 × 3/8-3/16 × 3/16
Miami Int. - C	USA	9L/27R	AC	T-DS	38 × 6 × 6	1 1/2 × 1/4 × 1/4
Miami Int. - C	USA	9R/27L	AC	T-DS	38 × 6 × 6	1 1/2 × 1/4 × 1/4
Patrick Henry Field - C	USA	6/24	PCC	T-PGWC	13 × 3 × 3	1/2 × 1/8 × 1/8
Peoria (Ill.) - C	USA	12/30	AC	T-DS	51-76 × 6 × 6	2-3 × 1/4 × 1/4
Savannah - C	USA	18/36	PCC	T-PGWC	N/A	N/A
South Bend - C	USA	9/27	AC	T-DS	32 × 6 × 6	1 1/4 × 1/4 × 1/4
St. Louis Lambert - C	USA	6/24	PCC	T-DS	32 × 6 × 6	1 1/4 × 1/4 × 1/4
Vance - M	USA	17R/35L	PCC	T-DS	51 × 6 × 6	2 × 1/4 × 1/4
Williamsport - C	USA	9/27	AC	T-DS	32 × 6 × 6	1 1/4 × 1/4 × 1/4

Table 9. Grooved runways constructed during 1973

Airport	Country	Runway	Surface	Grooving technique	Groove pattern, P × W × D	
					mm	in.
Albany (N.Y.) - C	USA	10/28	AC	T-DS	32 × 6 × 6	1 1/4 × 1/4 × 1/4
Allentown - C	USA	13/31	AC	T-DS	38 × 6 × 6	1 1/2 × 1/4 × 1/4
Bagotville - M	Canada	11/29	PCC	T-PGWC	N/A	N/A
Bangor - C	USA	15/33	PCC	T-DS	32 × 6 × 6	1 1/4 × 1/4 × 1/4
Cedar Rapids - C	USA	8/26	AC	T-DS	32 × 6 × 6	1 1/4 × 1/4 × 1/4
Cedar Rapids - C	USA	13/31	AC	T-DS	32 × 6 × 6	1 1/4 × 1/4 × 1/4
Chattanooga - C	USA	2R/20L	AC	T-DS	38 × 6 × 6	1 1/2 × 1/4 × 1/4
Chicago O'Hare - C	USA	14L/32R	AC	T-DS	32 × 6 × 6	1 1/4 × 1/4 × 1/4
Chicago O'Hare - C	USA	14R/32L	AC	T-DS	32 × 6 × 6	1 1/4 × 1/4 × 1/4
Chicago O'Hare - C	USA	9R/27L	AC	T-DS	32 × 6 × 6	1 1/4 × 1/4 × 1/4
Cleveland Hopkins - C	USA	10L/28R	AC	T-DS	38 × 6 × 6	1 1/2 × 1/4 × 1/4
England - M	USA	14/32	PCC	T-DS	51 × 6 × 6 (Skip 610)	2 × 1/4 × 1/4 (Skip 24)
Elsworth - M	USA	12/30	AC	T-DS	38 × 6 × 6	1 1/2 × 1/4 × 1/4
Harry S. Truman - C	USA	9/27	AC	T-DS	51 × 10 × 6	2 × 3/8 × 1/4
Jacksonville Int. - C	USA	7/25	AC	T-DS	51 × 6 × 6	2 × 1/4 × 1/4
John F. Kennedy - C	USA	13L/31R	AC	T-DS	38 × 10-5 × 5	1 1/2 × 3/8-3/16 × 3/16
John F. Kennedy - C	USA	4L/22R	PCC/AC	T-DS	38 × 10-5 × 5	1 1/2 × 3/8-3/16 × 3/16
Lawton - C	USA	17/35	PCC	T-PG	51 × 6 × 3	2 × 1/4 × 1/8
Los Angeles Int. - C	USA	6R/24L	PCC/AC	T-DS	38 × 6 × 6	1 1/2 × 1/4 × 1/4
Louisville - C	USA	1/19	PCC	T-PGWB	N/A	N/A
Memphis Int. - C	USA	17L/35R	PCC	T-PGWB	N/A	N/A
Minneapolis - C	USA	11R/29L	PCC/AC	T-DS	32 × 6 × 6	1 1/4 × 1/4 × 1/4
Newark - C	USA	4R/22L	AC	T-DS	38 × 10-5 × 5	1 1/2 × 3/8-3/16 × 3/16
Patrick Henry Field - C	USA	2/20	PCC	T-PGWC	13 × 3 × 3	1/2 × 1/8 × 1/8
Pittsburg - C	USA	10L/28R	PCC	T-DS	32 × 6 × 6	1 1/4 × 1/4 × 1/4
Ponca City - C	USA	17/35	PCC	T-PG	51 × 6 × 3	2 × 1/4 × 1/8
Washington Nat. - C	USA	18/36	AC	T-DS	32 × 6 × 6	1 1/4 × 1/4 × 1/4

Table 10. Grooved runways constructed during 1974

Airport	Country	Runway	Surface	Grooving technique	Groove pattern, P × W × D	
					mm	in.
Arlanda - C	Sweden	N/A	PCC	N/A	25 × 3 × 3	1 × 1/8 × 1/8
Beaumont - C	USA	11/29	PCC	T-PG	51 × 6 × 6	2 × 1/4 × 1/4
Boston Logan - C	USA	4L/22R	AC	T-DS	57 × 6 × 6	2 1/4 × 1/4 × 1/4
Boston Logan - C	USA	15R/33L	AC	T-DS	57 × 6 × 6	2 1/4 × 1/4 × 1/4
Cannon - M	USA	3/21	PCC	T-DS	51 × 6 × 6 (Skip 610)	2 × 1/4 × 1/4 (Skip 24)
Charlotte - C	USA	5/23	PCC/AC	T-DS	44 × 6 × 6	1 3/4 × 1/4 × 1/4
Chicago O'Hare - C	USA	9L/27R	AC	T-DS	32 × 6 × 6	1 1/4 × 1/4 × 1/4
Chicago O'Hare - C	USA	4L/22R	AC	T-DS	32 × 6 × 6	1 1/4 × 1/4 × 1/4
Denver Stapleton - C	USA	17L/35R	PCC	T-DS	51 × 6 × 6	2 × 1/4 × 1/4
Des Moines Mun. - C	USA	12L/30R	AC	T-DS	32 × 6 × 6	1 1/4 × 1/4 × 1/4
Dunedin - C	New Zealand	N/A	N/A	N/A	N/A	N/A
Elmira - C	USA	10/28	AC	T-DS	32 × 6 × 6	1 1/4 × 1/4 × 1/4
Erie - C	USA	6/24	AC	T-DS	51 × 6 × 6	2 × 1/4 × 1/4
Fort Lauderdale - C	USA	9L/27R	AC	T-DS	38 × 6 × 6	1 1/2 × 1/4 × 1/4
Grand Forks - M	USA	17/35	PCC	T-DS	51 × 6 × 6	2 × 1/4 × 1/4
Houston Int. - C	USA	14/32	PCC	T-PG	51 × 6 × 6	2 × 1/4 × 1/4
Invercargill - C	New Zealand	N/A	N/A	N/A	N/A	N/A
Kansas City Int. - C	USA	9/27	PCC	T-DS	32 × 6 × 6	1 1/4 × 1/4 × 1/4
Kansas City Int. - C	USA	1/19	PCC/AC	T-DS	32 × 6 × 6	1 1/4 × 1/4 × 1/4
Kincheloe - M	USA	15/33	PCC	T-DS	51 × 6 × 6	2 × 1/4 × 1/4
Knoxville - C	USA	4L/22R	PCC	T-PGWB	N/A	N/A
Lubbock Int. - C	USA	8/26	PCC	T-DS	32 × 6 × 6	1 1/4 × 1/4 × 1/4
Monroe (La.) - C	USA	4/22	PCC	T-PG	13 × 6 × 3	1/2 × 1/4 × 1/8
New Haven - C	USA	2/20	AC	T-DS	48 × 6 × 6	1 7/8 × 1/4 × 1/4
Pittsburg - C	USA	14/32	PCC/AC	T-DS	32 × 6 × 6	1 1/4 × 1/4 × 1/4
Pittsburg - C	USA	10R/28L	PCC	T-DS	32 × 6 × 6	1 1/4 × 1/4 × 1/4
San Antonio - C	USA	12R/30L	PCC	T-PG	51 × 6 × 6	2 × 1/4 × 1/4
Tallahassee - C	USA	18/36	AC	T-DS	44 × 6 × 6	1 3/4 × 1/4 × 1/4
Tampa - C	USA	18R/36L	AC	T-DS	44 × 6 × 6	1 3/4 × 1/4 × 1/4
Washington Nat. - C	USA	15/33	AC	T-DS	32 × 6 × 6	1 1/4 × 1/4 × 1/4
Wilkes-Barre - C	USA	4/22	AC	T-DS	38 × 6 × 6	1 1/2 × 1/4 × 1/4
Victoria Int. - C	Canada	N/A	N/A	N/A	N/A	N/A
Zurich - C	Switzerland	N/A	N/A	N/A	N/A	N/A

Table 11. Grooved runways constructed during 1975

Airport	Country	Runway	Surface	Grooving technique	Groove pattern, P × W × D	
					mm	in.
Albany County - C	USA	N/A	AC	T-DS	32 × 6 × 6	1 1/4 × 1/4 × 1/4
Boston Logan - C	USA	N/A	AC	T-DS	57 × 6 × 6	2 1/4 × 1/4 × 1/4
Cumberland (Md.) - C	USA	N/A	N/A	T-DS	N/A	N/A
Jackson County (W.Va.) - C	USA	N/A	AC	T-DS	32 × 6 × 6	1 1/4 × 1/4 × 1/4
Lihue (H.I.) - C	USA	N/A	AC	T-DS	44 × 6 × 6	1 3/4 × 1/4 × 1/4
NASA Kennedy - C	USA		PCC	T-DS	29 × 6 × 6	1 1/8 × 1/4 × 1/4
Raleigh Heights (W.Va.) - C	USA	N/A	PCC/AC	T-DS	32 × 6 × 6	1 1/4 × 1/4 × 1/4
Wood County (W.Va.) - C	USA	N/A	AC	T-DS	38 × 6 × 6	1 1/2 × 1/4 × 1/4

Table 12. Grooved runways constructed during 1976

Airfield	Runway	Surface	Touchdown area, rubber deposits			Trafficked, no rubber			Untrafficked, no rubber		
			SDR (a)	ATD		SDR (a)	ATD		SDR (a)	ATD	
				mm	in.		mm	in.		mm	in.
Travis	21L	PCC	5.79	0.3759	0.0148	2.28	0.9677	0.0381	----	----	----
Fairchild	23	PCC	4.75	.1092	.0043	1.97	.4318	.0170	1.97	0.2769	0.0109
Castle	30	AC	4.60	.1448	.0057	2.00	----	----	1.59	.8306	.0327
Loring	01	AC	4.58	.1499	.0059	1.99	.3632	.0143	----	----	----
Travis	21R	AC	4.01	.3632	.0143	2.71	.4140	.0163	2.18	.5537	.0218
McGuire	24	AC	3.92	.1575	.0062	1.93	.3073	.0121	1.33	----	----
Torrejon	23	AC	3.85	.1626	.0064	1.85	1.1633	.0458	1.50	.6452	.0254
Mather	22L	PCC/AC	3.75	.2083	.0082	1.86	.4140	.0163	----	----	----
Blytheville	17	PCC	3.73	----	----	2.45	----	----	1.57	----	----
Dover	01	PCC/AC	3.62	----	----	1.74	----	----	1.47	----	----
Scott	31	AC	3.61	----	----	1.83	----	----	1.47	----	----
Robbins	32	PCC	3.59	.2896	.0114	2.01	.4928	.0194	----	----	----
Cannon	21	PCC/GPCC	3.59	----	----	1.74	----	----	1.43	----	----
Rickenbacker	23L	PCC	3.40	.2769	.0109	2.04	.4851	.0190	1.86	.5055	.0199
Homestead	05	PCC	3.37	.2235	.0088	1.92	.7061	.0278	2.17	.4140	.0163
Grissom	22	AC	3.23	.1041	.0041	1.66	.5055	.0199	1.60	.5283	.0208
Charleston	15	AC/PCC	3.21	.2159	.0085	2.55	----	----	2.21	.3302	.0130
Zaragosa	31R	AC	2.93	.2591	.0102	1.31	.5817	.0229	1.32	.5537	.0218
Mather	22R	AC	2.90	.2083	.0082	2.18	.4140	.0163	1.67	----	----
Andrews	01L	PCC	2.89	.4064	.0160	2.14	.5588	.0220	2.28	.9398	.0370
Charleston	21	AC	2.79	.3327	.0131	1.88	.5817	.0229	----	----	----
Shaw	4L	PCC/GPCC/AC	2.77	.3429	.0135	1.79	.7264	.0286	1.52	.4851	.0191
McConnel	18R	AC	2.77	----	----	2.03	----	----	----	----	----
Hector	35	PCC	2.72	----	----	1.95	.6121	.0241	1.89	----	----
Dover	31	AC	2.66	----	----	1.89	----	----	1.28	----	----
Columbus	13L	PCC/AC	2.62	.4851	.0191	1.80	.4851	.0191	1.71	.5537	.0218
Glasgow	28	PCC	2.61	.3632	.0143	2.11	.2464	.0097	2.37	.1727	.0068
Andrews	01R	PCC/AC	2.60	.3302	.0130	1.73	.635	.025	1.82	.686	.027
England	14	PCC	2.54	----	----	2.66	.5055	.0199	----	----	----
Aviano	05	AC	2.51	.889	.035	1.73	1.168	.046	1.84	.965	.038
R. Gebaur	36	PCC/AC	2.50	----	----	2.22	----	----	2.29	----	----
Vance	17R	PCC/AC/GPCC	2.50	----	----	1.50	----	----	1.53	----	----
Soesterberg	28	AC	2.42	----	----	2.29	----	----	1.57	----	----
Columbus	13R	PCC	2.40	----	----	2.28	----	----	----	----	----
England	18	PCC/AC	2.39	.6452	.0254	2.57	.6375	.0251	2.40	----	----
Moody	18R	PCC/AC	2.38	.4851	.0191	1.48	1.1633	.0458	1.32	1.1633	.0458
Zweibrucken	03	AC	2.34	.5283	.0208	1.35	.8941	.0352	1.16	.7264	.0286
Bentwaters	25	PCC/AC	2.33	.4851	.0191	1.44	1.1633	.0458	1.57	.6121	.0241
Moody	18L	PCC/AC	2.32	.3073	.0121	1.66	.5283	.0208	1.45	.6121	.0241
Craig	32L	PCC/AC	2.27	.4318	.0170	1.70	.3327	.0131	1.42	1.3462	.0530
Rickenbacker	23R	AC	2.26	----	----	1.94	----	----	----	----	----
Vance	17C	PCC/AC	2.25	.1448	.0057	1.45	.8941	.0352	1.52	----	----
Columbus	13C	PCC/AC	2.22	----	----	1.90	----	----	2.13	----	----
Woodbridge	27	AC	2.22	----	----	1.53	----	----	2.01	----	----
Niagara Falls	28	AC	2.12	.1651	.0065	1.80	.4851	.0191	1.28	.6121	.0241
Vance	17L	PCC	2.10	----	----	2.09	.4851	.0191	----	----	----
McConnel	18L	AC	2.03	----	----	1.73	----	----	1.89	----	----
McGuire	36	PCC/AC	2.00	.1575	.0062	1.66	.3023	.0121	1.36	----	----
Myrtle Beach	17	PCC/AC	2.00	.4013	.0158	1.57	.5283	.0208	1.52	.6452	.0254
Cannon	30	PCC/AC	2.00	----	----	1.65	----	----	1.81	----	----
Shaw	04R	PCC/PGWC/PCC	1.99	.3150	.0124	1.13	1.5570	.0613	1.38	----	----
Erding	26	PCC	1.93	.2184	.0086	2.04	.4851	.0191	1.73	.4470	.0176
Hurlburt	35	PCC/AC	1.89	.5055	.0199	1.92	.6833	.0269	1.34	.8306	.0327
McChord	34	AC	1.87	.7747	.0305	2.23	.8306	.0327	2.13	.7747	.0305

[a] DBV SDR 3 minutes after wetting.

Table 13. DBV SDR and NASA grease test ATD obtained on runways evaluated July 1973 to December 1974 by AFCEC [From reference 28]

Airfield	Runway	Rubber-coated touchdown areas				Trafficked, no rubber (wheel paths)		Untrafficked, no rubber (runway edge)	
		Primary		Secondary					
		SDR (a)	Surface	SDR (a)	Surface	SDR (a)	Surface	SDR (a)	Surface
Palmdale	07/25	6.12	PCC	2.55	PCC	2.31	PCC	----	PCC/AC
March	13/31	5.19	PCC	2.46	PCC	2.21	PCC	----	AC
Barksdale	14/32	4.73	AC	3.70	AC	1.84	AC	1.40	AC
Norton	05/23	4.58	PCC	2.75	PCC	2.19	PCC	2.40	PCC
[b]Webb	17L/35R	2.95	PCC/AC	1.51	PCC/AC	4.51	AC	----	AC
Dyess	16/34	3.52	PCC	4.46	PCC	2.61	PCC	----	AC
Carswell	17/35	3.78	AC/PCC	4.11	PCC	2.36	AC/PCC	1.32	AC
Elmendorf	05/23	3.53	AC	1.92	AC	2.95	AC	1.52	AC
Reese	17R/35L	3.03	PCC	1.85	PCC/AC	1.80	PCC/AC	1.72	AC
Davis Monthan	12/30	2.98	AC	2.50	PCC	1.54	AC	1.39	AC
Palmdale	04/22	2.88	AC	2.43	AC	1.82	AC	2.05	AC
[b]Webb	17R/35L	2.82	PCC/AC	2.65	PCC/AC	2.69	AC	----	AC
Laughlin	13C/31C	2.70	PCC/AC	1.88	PCC/AC	1.69	AC	1.75	AC
Randolph	14L/32R	2.65	PCC	2.16	PCC	2.05	PCC	2.27	PCC
Yokota	18/36	2.61	PCC	1.95	PCC	1.91	PCC	1.94	PCC
Reese	17C/35C	2.37	AC	2.59	AC	2.15	AC	2.06	AC
Williams	12L/30R	2.52	PCC/AC	1.57	AC	1.68	AC	1.65	AC
[c]Williams	12C/30C	2.39	PCC	----	----	----	----	----	----
Williams	12R/30L	2.36	PCC	2.16	PCC	2.22	PCC	2.03	PCC
Laughlin	13L/31L	2.15	PCC/AC	2.31	PCC/AC	1.35	AC	----	AC
Elmendorf	15/33	2.21	AC	1.86	AC	2.05	AC/PCC	----	AC
Laughlin	13R/31L	1.87	AC	2.20	AC	1.56	AC	----	AC
Randolph	14R/32L	2.13	PCC/AC	1.90	PCC	1.48	PCC/AC	1.39	PCC/AC
[d]Vandenberg	12/30	1.59	AC	1.54	AC	1.60	AC	1.32	AC
Reese	17L/35R	----	PCC/AC	----	PCC/AC	1.39	AC	----	AC

[a]Average DBV SDR 3 minutes after wetting.

[b]Asphalt emulsion diluted with water applied to asphaltic concrete.

[c]Runway under construction.

[d]New runway surface.

Table 14. DBV SDR obtained on runways evaluated January to June 1975 by AFCEC [From reference 38]

Airport	Runway	Touchdown area, rubber deposits				Trafficked, no rubber (wheel path)	
		SDR (a)	Surface	SDR (a)	Surface	SDR (a)	Surface
St. Louis Int.	12R/30L	4.79	12R:AC	3.51	30L:AC	2.90	AC
	6/24	2.48	24:PCC	2.13	6:PCC	1.85	PCC
	12L/30R	1.93	30R:PCC	1.35	12L:WCPCC	1.81	PCC
	17/35	1.77	17:PCC	1.63	35:PCC	1.79	PCC
Miami Int.	9R/27L	4.44	9R:AC	2.88	27L:AC	1.81	AC
	9L/27R	2.88	9L:AC	1.98	27R:AC	1.72	AC
	12/30	2.01	12:AC	1.75	30:AC	1.56	AC
	17/35	1.35	17:AC	1.32	35:AC	1.33	AC
Memphis Int.	17L/35R	3.82	17:PCC	3.51	35R:PCC	2.44	PCC
	[b]9/27	1.83	27:AC	1.58	9:AC	1.32	AC
	[b]17R/35L	----	----	----	----	1.47	PCC
	3/21	1.18	3:AC	1.16	21:AC	1.17	AC
New Orleans Int.	10/28	3.76	10:PCC	2.22	28:AC	2.26	PCC
	1/19	3.22	19:PCC	3.03	1:AC	2.17	PCC
	5/23	1.22	23:AC	----	5:AC	1.32	AC
Atlanta W. B. Hartsfield	9L/27R	2.88	9L:WCPCC	2.26	27R:WCPCC	1.38	WCPCC
	15/33	2.21	33:AC	1.72	15:AC	1.50	AC
	9R/27L	2.09	27L:GPCC	1.24	9R:GPCC	1.12	GPCC
	3/21	1.69	21:AC	1.52	3:AC	1.36	AC
Jacksonville Int.	7/25	2.77	7:PCC	2.53	25:PCC	2.12	PCC
	13/31	2.65	31:PCC	2.33	13:PCC	1.97	PCC
Greater Cincinnati	18/36	2.45	36:AC	1.93	18:AC	1.73	AC
	9R/27L	2.38	27L:AC	2.09	9R:AC	1.77	AC
	9L/27R	1.30	9L:PCC	1.15	27R:PCC	1.25	PCC
Charlotte Douglas	18/36	2.32	36:AC	1.39	18:AC	1.46	AC
	5/23	1.81	5:AC	1.38	23:AC	1.22	AC
Nashville Int.	13/31	2.12	31:AC	1.71	13:AC	1.69	AC
	2L/20R	2.08	20R:GAC	1.82	2L:GAC	2.04	GAC
	2R/20L	1.30	20L:AC	----	2R:AC	1.24	AC
Charleston Kanawha	5/23	1.33	23:GPCC	1.10	5:GPCC	1.09	GPCC
	14/32	1.20	32:AC	1.09	14:AC	1.16	AC

[a]Average DBV SDR.

[b]New surface; under construction.

Table 15. DBV SDR obtained at 10 civil airports evaluated November 1971 to April 1972 by FAA [From reference 29]

Airport	Date tested	Runway	Rubber deposits	SDR		Surface; date installed	Groove pattern; date installed	Source
				DBV	Aircraft			
Cannon AFB	11/73	3/21	Heavy None	[a]3.59 to 2.46 1.74	—	305 m (1000 ft) PCC, 2438 m (8000 ft) GPCC, 305 m (1000 ft) PCC; date unknown	51 × 6 × 6 mm (2 × 1/4 × 1/4 in.), groove 610 mm (2 ft) skip 610 mm (2 ft); 1973	Reference 8
Shaw AFB	7/74	4L/27R	Med-lt None	2.77 to 1.97 1.79	— —	305 m (1000 ft) PCC, 1367 m (3500 ft) GPCC, 1370 m (4500 ft) GAC, 305 m (1000 ft) PCC; date unknown	51 × 6 × 6 mm (2 × 1/4 × 1/4 in.), groove 610 mm (2 ft) skip 610 mm (2 ft); 1971	Reference 8
Vance AFB	12/73	17R/35L	Lt-med None	[a]2.50 [a]1.50	—	457 m (1500 ft) PCC, 853 m (2800 ft) GPCC, 1036 m (3400 ft) AC; date unknown	51 × 6 × 6 mm (2 × 1/4 × 1/4 in.); 1973	Reference 8
Houston Int.	[b]6/70 10/71 2/25/71	8L/26R	Heavy-med Lt-none None Heavy	3.46 to 2.94 2.08 to 2.52 1.13 to 1.44 2.27 to 2.43	— [c]1.91 to 2.52 [d]1.10 to 1.53 —	PCC; date unknown	Ungrooved Ungrooved 51 × 6 × 6 mm (2 × 1/4 × 1/4 in.); 2/24/71	Unpublished Unpublished
Miami Int.	3/73 5/73 	9R/27L None 9L/27R 9R/27L 9R/27L 9L/27R	Heavy None Heavy-med Heavy-lt None None	4.62 to 3.51 2.43 3.16 to 2.38 2.42 to 1.51 1.51 1.22	— — — — — —	AC overlay; 11/72	Ungrooved 38 × 10 × 6 mm (1 1/2 × 1/4 × 1/4 in.); [e]1973	Unpublished Unpublished
John F. Kennedy	7/69 7/69 10/71	4R/22L	None Heavy Lt-none	1.75 2.20 1.47 to 1.80	[f]1.57 1.86 [c]1.50 to 1.67	PCC; 1959	38 × 10-5 × 3 mm (1 3/8 × 3/8-3/16 × 1/8 in.); 1967	Reference 1 Unpublished
Atlanta Int.	11/71	9R/27L	Heavy-med None	2.09 to 1.24 1.12	—	PCC; date unknown	32 × 10-3 × 6 mm (1 1/4 × 3/8-1/8 × 1/4 in.); 1969	Reference 10
Nashville Int.	4/72	2L/20R	Lt None	2.08 to 1.82 2.04	— —	AC; date unknown	32 × 6 × 6 mm (1 1/4 × 1/4 × 1/4 in.); 1970	Reference 10
Harry S. Truman	6/70	9/27	Heavy None Heavy None	2.28 1.40 1.69 1.18	— —	AC; date unknown	Ungrooved 38 × 6 × 6 mm (1 1/2 × 1/4 × 1/4 in.); 4/70	Unpublished
Seymour-Johnson AFB	7/69	8/26	None Heavy-lt	1.35 1.50	[f]1.38 1.47	PCC; 1960	51 × 6 × 6 mm (2 1/4 × 1/4 × 1/4 in.), groove 610 mm (2 ft) skip 610 mm (2 ft); 1968	Reference 1

[a] DBV test area contained both grooved and ungrooved pavements.

[b] Rubber removed after test.

[c] B-727.

[d] DC-9.

[e] 9L/27R being grooved at time of test.

[f] C-141.

Table 16. DBV and aircraft SDR obtained on transverse grooved runway surfaces with and without rubber contamination [From reference 39]

Airport	Runway	Surface (a)	Touchdown area, rubber deposits			Trafficked, no rubber		
			DBV SDR	ATD		DBV SDR	ATD	
				mm	in.		mm	in.
Allentown	13	GAC 1.0	1.07	1.56	0.061	1.08	1.48	0.058
	31		1.29	1.49	.059	1.08	1.48	.058
	6	GAC 0.75	2.07	1.52	.060	1.66	1.48	.058
	24		1.71	1.60	.063	1.66	1.48	.058
Akron-Canton	1	AC 1.4	2.71	0.229	0.009	2.01	0.305	0.012
	19		2.19	.229	.009			
	5	AC 1.4	1.32	.254	.010	1.47	.330	.013
	23		1.26	.330	.013			
Boston Logan	4L	GAC 1.0	1.12	---	---	0.90	---	---
	22R		1.00	---	---	.90	---	---
	4R	GAC 1.0	1.62	---	---	1.96	---	---
	22L		1.75	---	---	1.96	---	---
	15R	GAC 1.0	1.39	---	---	2.00	---	---
	33L		2.50	---	---	2.00	---	---
Buffalo	5	AC 1.0	2.06	0.838	0.033	2.30	0.864	0.034
	23		2.68	1.092	.043	2.30	.864	.034
	[b] 14							
	[b] 32							
Burlington	15	AC 1.0	2.09	0.559	0.022	1.75	0.584	0.023
	33		2.04	.508	.020			
Charleston, W.Va.	5	GPCC 0.8	1.27	0.211	0.008	1.35	0.221	0.009
	23		1.42	.165	.007			
	[b] 14							
	[b] 32							
Cincinnati	18	GAC 1.5	1.51	1.346	0.053	2.05	1.016	0.040
	36		1.70	1.270	.050			
	9R	GPCC 1.5	1.34	.838	.033	1.38	1.194	0.047
	27L		1.78	1.270	.050			
Cleveland	5R	GAC 1.3	1.7	0.737	0.029	2.14	1.092	0.043
	23L		2.4	.279	.011			
	10L	GAC 0.8	1.30	1.118	.044	1.57	1.702	.067
	28R		1.39	.737	.029			
Detroit	3L	GPCC 1.0	1.58	1.270	0.050	1.68	1.270	0.050
	21R		1.65	1.270	.050			
	9	PCC/AC 1.0	2.10	.432	.017	1.91	.508	.020
	27		2.77	.076	.003			
Dulles	1L	PCC 1.0	3.11	0.152	0.006	2.98	0.254	0.010
	19R		3.90	.102	.004			
	1R	PCC 1.0	4.48	.229	.009	3.13	.254	.010
	19L		3.12	.279	.011			
Ft. Wayne	4	PCC/AC 0.9	2.00	0.330	0.013	1.55	0.533	0.021
	22		2.05	.203	.008			
	9	PCC/AC N/A	1.77	1.016	.040	1.80	.508	.020
	27		1.81	.559	.022			
Grand Rapids	8R	PCC/AC 1.5	2.36	0.254	0.010	1.57	0.127	0.005
	26L		1.96	.254	.010			
Madison	18	PCC 1.5	1.68	0.686	0.027	1.43	1.016	0.040
	36		1.35	1.118	.044			
	13	AC 1.5	1.62	.381	.015	1.54	.127	.005
	31		1.70	.254	.010			

[a] Number on right of column represents the runway transverse slope in percent.

[b] Under construction.

Table 17. DBV SDR and NASA grease test ATD obtained on runways evaluated by the FAA trial application — runway friction calibration and pilot information program during August and September 1975

Airport	Runway	Surface (a)	Touchdown area, rubber deposits			Trafficked, no rubber		
			DBV SDR	ATD		DBV SDR	ATD	
				mm	in.		mm	in.
Milwaukee	[b]1L [b]19R							
	7R 25L	PCC 1.0	1.67 3.02	0.838 1.118	0.033 .044	1.56	0.432	0.017
Moline	9 27	AC 1.0	2.34 2.77	0.508 .102	0.020 .004	2.65	0.508	0.020
	12 30	PCC 1.0	2.66 2.91	.216 .152	.009 .006	2.49	.127	.005
Peoria	30 12	GAC 1.25	1.36 1.52	0.965 .991	0.038 .039	1.16	1.397	0.055
	4 22	AC 1.0	1.14 1.44	.635 .305	.025 .012	1.43	1.270	.050
Philadelphia	9R 27L	AC 1.0	4.99 3.57	0.127 .127	0.005 .005	2.47	0.279	0.011
Pittsburg	10R 28L	GAC 1.0	2.15 2.54	1.549 1.549	0.061 .061	1.63	1.600	0.063
	10L 28R	GAC 1.5	1.43 1.49	1.549 1.626	.061 .064	1.35	1.600	.063
Portland, Maine	11 29	AC 1.0	1.54 1.41	0.737 .762	0.029 .030	1.27	0.737	0.029
	18 36	AC 1.0	1.86 1.83	.254 .279	.010 .011	1.77	.279	.011
Rochester, N.Y.	10 28	AC 1.0	1.74 2.18	0.559 .178	0.022 .007	1.79	0.356	0.014
	4 22	PCC 1.0	3.68 4.50	.102 .127	.004 .005	3.60	.152	.006

[a]Number on right of column represents the runway transverse slope in percent.

[b]Under construction.

Table 17. Concluded

Year	Airport	Runway
1970	Hahn AB - M	11/29
	RAF Milden Hall - M	1/29
	Wiesbaden AB - M	8/26
1971	Dallas NAS - M	17/35
	Gallup (N. Mex.) - C	6/24
1972	Denver Stapleton - C	8L/26R
	Denver Stapleton - C	8R/26L
	Great Falls Int. - C	16/34
	Hot Springs (Va.) - C	6/24
	Nashville Metro. - C	2L/20R
	Sioux Falls (N. Dak.) - C	15/33
	Springfield (Mo.) - C	13/31
	Vernal (Utah) - C	16/34
	Wichita Mun. - C	N/A
1973	Bellingham (Wash.) - C	16/34
	Cedar City (Utah) - C	2/20
	Pease AFB - M	16/34
	Portland (Maine) - C	11/29
	RAF Alconbury - M	12/30
	Rapid City (S. Dak.) - C	14/32
	Ramstein AB - M	9/27
	Salt Lake City (Utah) - C	16L/34R
	Salt Lake City (Utah) - C	16R/34L
1973	St. Louis Lambert - C	6/24
1974	Aberdeen (S. Dak.) - C	13/31
	Farmington (N. Mex.) - C	7/25
	Greensboro-High Point - C	14/32
	Hill AFB - M	14/32
	Las Vegas (Nev.) - C	7/25
	RAF Bentwaters - M	7/25
	RAF Lakenheath - M	6/24
	Roswell (N. Mex.) - C	17/35
	Sioux City (Idaho) - C	17/35
1975	Boise (Idaho) - C	10R/28L
	Jackson Hole (Wyo.) - C	18/36
	Jamestown (N. Dak.) - C	12/30
	Las Vegas (Nev.) - C	1R/19L
	Missoula (Mont.) - C	11/29
	Monroe (La.) - C	4/22
	Pierre (S. Dak.) - C	13/31

Table 18. U.S. porous asphalt runway surface construction